Echoes and Delays: Time-to-build in Production Networks*

Edouard Schaal
CREI, ICREA, UPF, BSE and CEPR

Mathieu Taschereau-Dumouchel
Cornell University

February 2025 – Preliminary and Incomplete

Abstract

We study how time-to-build and delivery lags affect the propagation of sectoral and aggregate shocks in an economy with input-output linkages. Time-to-build significantly contributes to the persistence of shocks, with highly heterogeneous effects across sectors. We analyze delay shocks and demonstrate that bottlenecks can be identified by the product of a sector's supplier and buyer centralities. Shocks propagate asynchronously through the network, generating endogenous fluctuations via an *echo* effect. These fluctuations arise due to the presence of loops in the network. We show that the Fourier spectrum of sectoral and aggregate output can be predicted from the durations and weights of the network's dominant cycles. Sectoral comovements are complex and can be decomposed into the network's dominant walks.

JEL Classification: C67, D57, D85, E23, E32

*E-mail: eschaal@crei.cat, mt763@cornell.edu. Edouard Schaal acknowledges financial support from the Spanish Ministry of Economy and Competitiveness, through the Severo Ochoa Programme for Centres of Excellence in R&D (SEV-2015-0563 and CEX2019-000915-S) and through the program Proyecto I+D Excelencia 2017 (ECO2017-87827-P-AEI/FEDER, UE), and support from the Generalitat de Catalunya, through CERCA and SGR Programme (2017-SGR-1393).

1 Introduction

Firms in a modern economy rely extensively on goods and services produced by other suppliers. The time required to produce these intermediate inputs varies dramatically across industries. While some inputs, like components for furniture assembly or readily deliverable services, can be produced rapidly, others necessitate significantly longer production cycles. Building large transport vessels like container ships, for example, typically takes one to two years from order to delivery. Specialized energy infrastructure such as offshore oil rigs can have even longer lead times. Kydland and Prescott (1982) propose a model of business cycle fluctuations in a representative firm economy with time to build but without production networks.

This variation in time-to-build has important consequences for how economic shocks are transmitted through the production network. While shocks propagate rapidly along paths involving firms with short production times, they can take years to progress through firms with longer build times. When aggregated, this asynchronous propagation shapes the persistence of macroeconomic quantities. The network structure of the economy and the time-to-build distribution therefore influence the time series properties of GDP. As an extreme example, cycles in the production network, as they create paths for shocks to return to their originating firms, can give rise to recurring business cycle fluctuations.

Our work is motivated by evidence from the U.S. Census Bureau and Compustat which show large variations in *backlog ratios*, that is the time it would take for a firm to complete its outstanding orders at the current level of production. For instance, this backload ratio indicator shows that the "Printing ink manufacturing" sector fulfills orders almost immediately (0.15 months), while the equivalent number for the "Guided missile and space vehicle manufacturing" sector is two years. In addition, input-output tables provided by the Bureau of Economic Analysis show that the U.S. production network is replete with cycles of different lengths. As our analysis shows, these cycles can generate recurring fluctuations in economic activity.

We extend the classical framework of Long and Plosser (1983) by introducing heterogenous time-to-build into an otherwise standard multisector economy. Firms in the model use labor and intermediate goods as inputs and are subject to productivity shocks. Crucially, and in stark contrast with the prevalent roundabout framework, it takes time for goods to be produced. We also allow for heterogeneity across firms in this time-to-build dimension. Since production takes time, the response of the economy to a shock can be delayed. For instance, a shock to a sector with a lengthy production process will only affect that sector's output after a few periods. Other producers that rely on the output of the affected sector will see their own production respond with an additional delay, and so on, as we move further in the production network. Input-output linkages thus imply that delays compound along supply chains.

We consider a competitive equilibrium in this setup. Since markets are complete and that

there are no externalities, this equilibrium is efficient, and we therefore focus on the recursive problem of a social planner. We show that the value function associated with this problem can be written in closed-form. Building on this result, we provide a version of Hulten's (1978) theorem for network economies with heterogenous time-to-build. We show that the impact of a marginal increase in a sector's productivity on welfare is proportional to a time-adjusted version of that sector's Domar weight. This time adjustment captures how production delays postpone the time at which productivity shocks materialize.

To understand how time-to-build affects the persistence of shocks in the economy, we introduce a measure of a shock's *average duration* which captures how long it takes for output across sectors to respond to a disturbance. We show that we can decompose this average duration as the sum of multiple adjustment iterations. Intuitively, a shock to a sector triggers a response of its output with a delay that corresponds to its production time. This change in output then triggers a second round of adjustment that takes place through all of that sector's customers. Once again, production times matter, and the time it takes for these customers to produce their goods matters for the average duration of the shock. This process then goes through additional rounds, with decaying intensities. Our average duration measure also allows us to identify bottleneck sectors, those with large seller and buyer centralities. Those sectors play an important role in supply chains, and we show that any marginal increase in their production times lead to large increases in the persistence of shocks.

Exploring further the implications of heterogeneous time-to-build for the dynamic properties of the economy, we study the eigenvalues of the dynamic system described by the model. In the Long and Plosser (1983) benchmark, the eigenvalues are small and mostly real, indicating that after a shock the economy return rapidly and monotonously to its steady state. In contrast, in our full model eigenvalues are much larger and feature an important imaginary component. As a result, one-time shocks can have long-lasting effects and generate recurrent cycles.

We then turn to the model ability to generate oscillations, which we define as a recurring change in sectoral output. Two ingredients are necessary to generate oscillations: 1) non-zero production times, and 2) cycles in the production network. We show that when both ingredients are present, a shock can generate recurring fluctuations in economic activity. Cycles are therefore absent from roundabout production networks or those with purely vertical supply chains.

We rely on Fourier analysis to characterize how the structure of the production network and the distribution of production times affect the time series properties of sectoral output. One of our main results describes how cycles in the production network contribute to the Fourier spectrum, which describes the set of frequencies at which economic activity oscillates. Our decomposition result shows that the *durations* (i.e., total production times) and *weights* (i.e., the product of input shares) of the network's cycles shape the frequencies at which output oscillates. Applying this decomposition to the U.S., our findings indicate that the network's cycles virtually account for the entirety of the model-implied sectoral output spectrum.

Moving from the individual sectors to the cross-sectoral behavior of the economy, we show that the combination of heterogeneous time-to-build and input-output linkages generate complex dynamic comovements across sectors, which we illustrate with various examples of multi-sector impulse response functions. Echoing our spectral decomposition at the sectoral level, we show that comovements between sectors at any given lags can be decomposed into the network's *dominant walks*. Aggregating across sectors, we show that oscillations persist in the aggregate and characterize the Fourier spectrum of aggregate GDP into a within-sector component, accounted for by the network's dominant cycles, and a cross-sector component, governed by the network's dominant walks.

Literature Review

Our work extends the classical work of Long and Plosser (1983) in which firms are interconnected through production networks and take one period to produce, such that inputs use today contribute to output next period. We generalize this setup to include heterogenous production times across firms. One of our main findings is that this generalization allow richer dynamic patterns to arise. We also use Fourier analysis to describe how the structure of the production network affect the time series properties of economic variables.

Our work also relates to a large literature that studies how shocks propagate through production networks. In an influential paper, Acemoglu et al. (2012) explores how idiosyncratic shocks can given rise to large aggregate fluctuations through their propagation over in input-output linkages. Acemoglu et al. (2017) and Baqaee and Farhi (2019a) describe how network interactions can generate thick-tailed aggregate output distributions. Another strand of work that includes Jones (2011), Baqaee and Farhi (2019b) and Liu (2019) has studied the impact of distortions in production network economies. These papers, as well as the bulk of the literature, considers static models with roundabout production networks. In that setup, all transactions occur in a single period, so that producers effectively use their own output as an input. In contrast, production in our setup takes time which leads to cycles and persistent fluctuations.

Two papers are closer to our work. Liu and Tsyvinski (2024) study a framework in which firms must pay a cost for changing inputs. As a result, decisions become dynamic and shocks can have persistent effects. Carvalho and Reischer (2021) explore aggregate persistence in a network economy with one-period time-to-build, as in Long and Plosser (1983). They show that the economy aggregates to an ARMA process and explore how the process' coefficients depend on the production network. In contrast to both of their setups, we introduce heterogenous time-to-build in an otherwise business cycle framework. We also rely on Fourier analysis to explore how the structure of the network affects the time series properties of the economy.

We also relate to a literature, pioneered by Benhabib and Nishimura (1979), that shows that

limit cycles can emerge in the multi-sector neoclassical growth model with multiple stocks of capital. In contrast to capital, intermediate inputs in our model are short-lived, and the cycles that emerge through production network linkages always die out over time.

Our work is theoretical, but an empirical literature in trade argues that shipping times and delays are important. Djankov et al. (2010) find that an extra day of delay reduces trade by at least 1 percent. Hummels and Schaur (2013) estimate that an extra transit day is equivalent to a tariff that can be as high as 2 percent. Alessandria et al. (2023) study the impact of supply chain delays during the COVID pandemic.

The rest of this paper is organized as follows. The next section provides an overview of time-to-build in the U.S. data. The following section presents the model and derives its closed-form solution. In Section 4, we study how delivery time contribute to shock propagation and identify bottlenecks sectors. Section 5 describes how cycles in the production network can create cycles in sectoral time series, and Section 6 provides a similar analysis for sectoral comovements and the aggregate economy. We provide a quantitative illustration of the mechanisms of the model in Section 7. The last section concludes.

2 Data

To illustrate the implications of time-to-build in production networks, we examine intersectoral linkages in the U.S. economy. Throughout the paper, we use the 2017 Supply-Use Input-Output tables from the Bureau of Economic Analysis (BEA). The 2017 table represents the most recent data available with 402 industries at the 6-digit level. After excluding government-related sectors, we iteratively remove other sectors whose goods are neither consumed nor used as intermediates, leaving us with 372 sectors.

A common approach to measuring time-to-build is to consider *backlog ratios* (Liu and Tsyvinski, 2024). We define the backlog ratio for each industry as the average ratio of the stock value of unfilled orders over the flow value of goods delivered in a period. This measure reflects the number of periods it would take for an industry to fulfill all its outstanding orders at the current level of production. Although the ratio fluctuates over time due to seasonality and cyclical forces, its long-term average serves as a proxy for the time required to produce in a given industry.[1] We construct this measure using two different sources. The U.S. Census Manufacturers' Shipments, Inventories and Orders (M3) survey provides monthly statistical data allowing us to compute the average backlog ratio over the period 1992 to 2024. The dataset is broad-based and includes nearly all manufacturing companies with more than $500 million annual shipments but is restricted to the manufacturing sector and aggregated to 10 subsectors. We also use Standard and Poor's Compustat database,

[1] In the steady-state of our model, the backlog ratio is exactly equal to the duration between the time when production is initiated and final delivery.

whose Order Backlog variable allows us to construct the backlog ratio over the period 1970-2024. We convert the annual series into monthly data and compute the average within each 6-digit NAICS sector. The Compustat dataset only includes publicly-listed firms, but offers a more disaggregated and broader sectoral coverage.

Figure 1 shows the distribution of backlog ratios in months of production across sectors. The average backlog ratio is 5.38 months in the Census and 5.08 months in Compustat. As the figure shows, there is a large heterogeneity across sectors. Some sectors have very low backlog ratios and can fulfill their outstanding orders within a month, but backlogs can go up to 2 or 3 years in other sectors.[2] The peak is observed around 2-3 months for the Census (manufacturing only) and 5-6 months in Compustat.

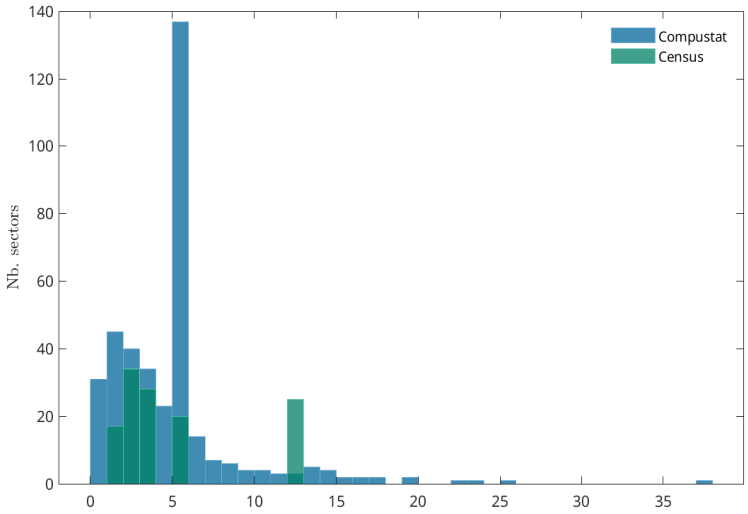

Figure 1: Distribution of backlog ratios in months across 6-digit sectors

3 Model

To understand the most fundamental ways in which time-to-build and delays affect the propagation of shocks in a production network, we build on the frictionless benchmark of Long and Plosser (1983) (LP83 hereafter), to which we introduce heterogeneity in delivery lags.

3.1 Notation

In what follows, we use bold notation for vectors and matrices. In the case of a column vector $\mathbf{x}$, x_i denote its ith-row element. In the case of a matrix $\mathbf{M}$, M_{ij} denote its element in the ith row

[2]Some examples of the lowest backlog ratios include 0.15 for "Printing ink manufacturing" and 0.24 for "Sugar and confectionery product manufacturing". Other examples of the largest backlogs include 24.0 months for "Guided missile and space vehicle manufacturing" or 25.5 for "Facilities support services" (Compustat).

and jth column. If $\mathbf{x}$ an $N \times 1$ column, the matrix $\mathbf{diag}(\mathbf{x})$ is the $N \times N$ diagonal matrix whose (i,i)th element is x_i. If a is a real number and $\mathbf{x}$ an $N \times 1$ column vector, $a^{\mathbf{x}}$ is the column vector $(a^{x_1}, \ldots, a^{x_N})'$. $\mathbf{I}_N$ is the $N \times N$ identity matrix. $\mathbf{1}$ is an $N \times 1$ vector with ones in each row and $\mathbf{1}\{\text{condition}\,(i)\}$ is an indicator vector with ith element equal to 1 when condition(i) is satisfied, 0 otherwise. Finally, we denote by $\boldsymbol{\delta}_i$ the $N \times 1$ vector whose ith element is 1 and all other rows are 0.

3.2 Environment

Time is discrete. There are N goods, each produced by a competitive sector. An infinitely-lived representative household maximizes its expected discounted utility over the consumption of the N goods:

$$E \sum_{t=0}^{\infty} \beta^t U\left(c_{1t}, \ldots, c_{Nt}\right),$$

where $0 < \beta < 1$ is the discount factor and c_{nt} is the quantity of good n consumed at time t. The household is endowed with one unit of labor which is supplied inelastically to firms.

Firms in sector $n = 1, \ldots, N$ operate the production technology

$$y_{nt} = A_{nt} F_n\left(l_{nt}, x_{n1,t}, \ldots x_{nN,t}\right), \tag{1}$$

where A_{nt} is sector n's total factor productivity (TFP), l_{nt} is the labor it employs and $x_{nm,t}$ is the amount of intermediate inputs it purchases from sector m at time t. The vector of sector-specific productivities $\{A_{nt}\}_{n=1}^N$ follows a first-order Markov chain that we later define more specifically. Importantly, production takes time: we model time-to-build as *delivery lags*. We assume that it takes τ_n periods before goods produced in sector n can be delivered either to the household for direct consumption or to other firms for their own production. We denote $X_{n\tau}$ the aggregate amount of good n scheduled for delivery τ periods from now.

3.3 Planning problem

Markets are complete and operate under perfect competition. Under the assumption that U is neoclassical, the economy is efficient and we solve the planning problem.

We write the planning problem recursively. Because of the delivery lag structure, its state variables include the entire vector of goods from sector i scheduled for delivery from today up to $\tau_n - 1$ periods from now, $\{X_{n\tau}\}_{\tau=0}^{\tau_n - 1}$. The planning problem can be written as

$$V\left(\{A_n\}_{n=1}^N, \{X_{1\tau}\}_{\tau=0}^{\tau_1-1}, \ldots, \{X_{N\tau}\}_{\tau=0}^{\tau_N-1}\right) = \max_{c_n, l_n, x_{nm}, y_n} U\left(c_1, \ldots, c_N\right) + \beta E\left[V\left(\{A'_n\}_{n=1}^N, \{X'_{1\tau}\}_{\tau=0}^{\tau_1-1}, \ldots, \{X'_{N\tau}\}_{\tau=0}^{\tau_N-1}\right)\right]$$

subject to the production functions (1) and the constraints, for all $1 \leq n \leq N$:

$$\sum_{n=1}^{N} l_n \leq 1, \tag{2}$$

$$c_n + \sum_{m=1}^{N} x_{mn} \leq X_{n0}, \tag{3}$$

$$X'_{n\tau} = X_{n\tau+1} \text{ for } 0 \leq \tau < \tau_n - 1 \tag{4}$$

$$X'_{n\tau_n-1} = y_n, \tag{5}$$

Equation (2) ensures that total employed labor does not exceed the endowment of time. Equation (3) is the resource constraint on good n delivered today, which must be either consumed or used as an intermediate inputs. Equations (4) and (5) provide the law of motion for the inventories of goods $X_{n\tau}$ to be delivered in the future. Specifically, the quantity of good n produced today, that will be delivered τ_n periods from now, appears in the inventories to be delivered $\tau_n - 1$ periods from tomorrow.

3.4 Analytical solution

The need to track the inventories of goods to be delivered in the future renders the planning problem intractable for many real-world applications (e.g., thousands of state variables when using the BEA's input-output tables). Fortunately, under a particular parametrization, the economy admits a closed-form solution: under the assumption that U is logarithmic and F is Cobb-Douglas, income and substitution effects cancel out, ensuring that the shares of consumption, intermediate inputs and labor remain fixed. In other words, despite the presence of heterogeneous time-to-build across sectors, quantities evolve in fixed proportion to the aggregate supply of goods, allowing one to derive analytical solutions for the economy's equilibrium objects.

We therefore assume from now on that preferences are logarithmic:

$$U(c_1, ..., c_N) = \sum_{n=1}^{N} \gamma_n \log c_n, \; \gamma_n \geq 0, \; \sum_{n=1}^{N} \gamma_n = 1, \tag{6}$$

and that the production function F_n is Cobb-Douglas with constant returns-to-scale

$$F_n(l, x_1, ..., x_N) = l^{\alpha_n} \prod_{m=1}^{N} x_{nm}^{\omega_{nm}}, \quad \alpha_n + \sum_{m} \omega_{nm} = 1, \tag{7}$$

and we denote $\mathbf{\Omega}$ the matrix of intermediate input shares, such that $[\mathbf{\Omega}]_{nm} = \omega_{nm}$. Proposition 1 below summarizes the results behind the analytical solution:

Proposition 1. *Under assumptions (6) and (7), the planner's value function can be expressed as*

$$V\left(\{A_n\}_{n=1}^N, \{X_{1\tau}\}_{\tau=0}^{\tau_1-1}, \ldots\right) = \sum_{n=1}^{N}\sum_{\tau=0}^{\tau_n-1} \beta^\tau \zeta_n \log X_{n\tau} + G\left(\{A_n\}_{n=1}^N\right) + \kappa$$

where

$$\boldsymbol{\zeta} = \left(\mathbf{I} - [\boldsymbol{\Omega}\boldsymbol{diag}(\beta^{\boldsymbol{\tau}})]'\right)^{-1}\boldsymbol{\gamma} \tag{8}$$

$$G\left(\{A_n\}_{n=1}^N\right) = \sum_n \beta^{\tau_n}\zeta_n \log A_n + \beta E\left[G\left(\{A_n'\}_{n=1}^N\right)\right] \tag{9}$$

and the allocation satisfies

$$\begin{aligned} c_n &= \overline{c_n} X_{n0} \\ x_{nm} &= \overline{x_{nm}} X_{n0} \\ l_n &= \overline{l_n}, \end{aligned}$$

where $\overline{c}_n$, $\overline{x}_{nm}$, $\overline{l}_n$ and κ are constants, whose expressions can be found in Appendix B.

This result establishes that under log preferences and Cobb-Douglas production the planner's value function is logarithmic. Specifically, it depends on two main components: one related to the stock of inventories $\{X_{n\tau}\}$ and one associated with productivity $\{A_n\}$. The inventory component shows that, unsurprisingly, the household discounts goods that become available further in the future more heavily through β^τ. Different goods also contribute differently to welfare, as captured by the weights $\{\zeta_n\}$. Equation (8) makes clear that the household prefers goods that are 1) important in the utility bundle (high γ_n), or 2) are important (direct or indirect) inputs in the production of goods with high γ. This last channel is captured by the modified Leontief inverse $\left(\mathbf{I} - [\boldsymbol{\Omega}\mathbf{diag}\,(\beta^{\boldsymbol{\tau}})]'\right)^{-1}$. Unlike in static models ($\tau = 0$), the discount rate β plays a role here, so that a good n has a greater social value (high ζ_n) if it used in the production of goods with short time-to-build. Those are the goods that are enjoyed quickly by the household, and so their contribution to welfare is less discounted.

We can get further intuition into ζ by taking advantage of the link between the equilibrium allocation and the planner's problem. Setting prices equal to their marginal welfare value, we can define the spot price of good n for immediate delivery as[3]

$$p_n = \frac{\partial V}{\partial X_{n0}} = \frac{\zeta_n}{X_{n0}}.$$

Using that definition, ζ coincides with the vector of Domar weights, as the following result shows.

[3]We refer the reader to the the proof of Proposition 1 in the Appendix for an expression of the wage.

Lemma 1. *The coefficients ζ_n are equal to the consumption-time adjusted Domar weights,*

$$\zeta_n = \frac{p_{nt} y_{nt-\tau_n}}{VA_t},$$

where $VA_t = \sum p_{nt} c_{nt}$ is aggregate value added.

As usual, the Domar weights are simply the shares of a good's sales in nominal GDP (recall that $y_{nt-\tau_n}$ is the amount of good n that becomes available at t). Figure 11 in the Appendix displays the model-implied Domar weights.

The household's value function also depends on the productivity component $G(\{A_n\})$, which is described by the recursive equation (9).[4] We can use the envelope theorem to get further insight in how A_n affect welfare. Assuming temporarily that the TFP shocks A_{nt} are iid, we find that

$$\frac{\partial V}{\partial \log A_n} = \beta^{\tau_n} \zeta_n. \tag{10}$$

Intuitively, the impact of a productivity shock A_n only materializes τ_n periods later, which explains the discounting. The Domar weight ζ_n, as it summarizes the impact of the shock on aggregate value added at $t + \tau_n$, also plays a role. Expression (10) is the equivalent of Hulten's (1978) theorem in our setting, and shows that the theorem must be adjusted to take into account that production is not immediate.

Finally, the last part of Proposition 1 shows that the household consumes a constant share $\overline{c_n}$ of the available stockX_{n0} of good n and that the remainder is used as intermediate input for production. The Cobb-Douglas production function and the fixed supply of labor also imply that the amount of labor assigned to each sector is constant.

3.5 Output Dynamics

The dynamics of output in each sector are straightforward to compute, thanks to the fixed share result: $y_{nt} = A_{nt} \overline{l}_n^{\alpha_n} \prod_m (\overline{x}_m y_{m,t-\tau_m})^{\omega_{nm}}$. Assuming that the TFP process is stationary with mean $E[A_n] = A_n^{ss}$, we evaluate sectoral output in log-deviation from the nonstochastic steady state in which all productivities are held constant at their mean:

$$\hat{y}_{nt} = \hat{A}_{nt} + \sum \omega_{nm} \hat{y}_{m,t-\tau_m}, \tag{11}$$

where $\hat{x} = \log x - \log x^{ss}$ and x^{ss} is the value of variable x in the nonstochastic steady state. In other words, the vector of sectoral outputs $\hat{\mathbf{y}}_t$ follows the VAR(τ_{max}) process

$$\hat{\mathbf{y}}_t = \mathbf{\Omega}_1 \hat{\mathbf{y}}_{t-1} + \ldots + \mathbf{\Omega}_{\tau_{max}} \hat{\mathbf{y}}_{t-\tau_{max}} + \hat{\mathbf{A}}_t \tag{12}$$

[4] So far we have only assumed that $\{A_i\}$ follows a first-order Markov process. With additional assumptions we can often characterize G in closed-form.

where $\mathbf{\Omega}_\tau = \mathbf{\Omega}\mathbf{diag}\left(\mathbf{1}\left\{\tau = \tau_i\right\}\right)$ and $\mathbf{1}$ is an indicator vector and $\tau_{max} = \max_n \tau_n$.

The framework nests two well-known cases:

1. **Roundabout production**. This case is the most studied version in the literature and corresponds to having no time-to-build ($\tau_n = 0$). The output vector satisfies the equation $\hat{\mathbf{y}}_t = \mathbf{\Omega}\hat{\mathbf{y}}_t + \hat{\mathbf{A}}_t$, which yields the well-known Leontief inverse (Acemoglu et al., 2012):

$$\hat{\mathbf{y}}_t = (\mathbf{I} - \mathbf{\Omega})^{-1} \hat{\mathbf{A}}_t = \hat{\mathbf{A}}_t + \mathbf{\Omega}\hat{\mathbf{A}}_t + \mathbf{\Omega}^2\hat{\mathbf{A}}_t + \dots \tag{13}$$

   This equation shows that the output vector can be expressed as the sum of the direct effects of the productivity shocks on each sector ($\hat{\mathbf{A}}_t$) and all the higher-order effects through multiple rounds of the production networks ($\mathbf{\Omega}\hat{\mathbf{A}}_t + \mathbf{\Omega}^2\hat{\mathbf{A}}_t + \dots$).

2. **Long and Plosser (1983)**. This version of the model assumes $\tau_n = 1$. In this case, equation (12) becomes

$$\hat{\mathbf{y}}_t = \mathbf{\Omega}\hat{\mathbf{y}}_{t-1} + \hat{\mathbf{A}}_t = \hat{\mathbf{A}}_t + \mathbf{\Omega}\hat{\mathbf{A}}_{t-1} + \mathbf{\Omega}^2\hat{\mathbf{A}}_{t-2} + \dots \tag{14}$$

   Here, the output vector follows a VAR(1) with an MA representation that expresses the output vector at time t as the sum of the impacts of contemporaneous productivity shocks ($\hat{\mathbf{A}}_t$) and past shocks, compounded with the corresponding number of iterations of the production network $\left(\mathbf{\Omega}^k\hat{\mathbf{A}}_{t-k}\right)$.

4 Persistence and Delays

The introduction of time-to-build in production networks has significant implications for the persistence of shocks. In this section, we introduce a persistence statistic to assess how delivery times in different sectors influences shock propagation. We then explore delay shocks and identify sectors that act as bottlenecks in this process.

To focus on the propagation effects driven by time-to-build and intersectoral linkages solely, we eliminate other sources of persistence and assume that productivity shocks are *i.i.d.* from this section to Section (6).

4.1 Persistence

A natural consequence of time-to-build is to make shocks more persistent, as disruptions in one industry take time to affect both immediate and distant downstream sectors. However, the degree of persistence depends on the structure of the production network and the specific time-to-build within each sector. We introduce a simple persistence statistic that can be computed analytically to determine the average duration of a shock. Additionally, we use this statistic to identify bottleneck sectors—those where delays significantly amplify the persistence of aggregate shocks in the economy.

Denote by $\hat{\mathbf{y}}_t\left(\hat{\mathbf{A}}\right)$ the vector of impulse responses of output in each sector at time t to a particular combination of shocks $\hat{\mathbf{A}} \geq 0$ at time 0, starting from the steady state. We define the *average duration* of a shock as

$$\mathcal{T}_{\mathbf{w}}\left(\hat{\mathbf{A}}\right) = \sum_{\tau=0}^{\infty} \sum_{n} \tau w_n \hat{y}_{n\tau}\left(\hat{\mathbf{A}}\right), \tag{15}$$

where $\mathbf{w} \geq 0$ is a vector of sectoral weights. We can interpret $\mathcal{T}_{\mathbf{w}}$ as the expectation of a random variable which takes value τ with probability $\sum_n w_n \hat{y}_{n\tau}\left(\hat{\mathbf{A}}\right)$. The longer a shock persists (i.e., higher amplitude of the impulse response at high τ), the higher the average duration $\mathcal{T}_{\mathbf{w}}$. Note, for instance, that $\mathcal{T}$ is exactly 0 in the roundabout production case with iid shocks. Since the response of the economy is linear and scales up with the size of the shocks, we normalize the shocks to 1 for the purpose of cross-sectoral comparisons.

Proposition 2. *The average duration* $\mathcal{T}_{\mathbf{w}}\left(\hat{\mathbf{A}}\right)$ *for weighting vector* $\mathbf{w} > 0$ *is*

$$\mathcal{T}_{\mathbf{w}}\left(\hat{\mathbf{A}}\right) = \mathbf{w}'\boldsymbol{\Omega}\left(\mathbf{I} - \boldsymbol{\Omega}\right)^{-1} \boldsymbol{diag}\left(\boldsymbol{\tau}\right)\left(\mathbf{I} - \boldsymbol{\Omega}\right)^{-1} \hat{\mathbf{A}}. \tag{16}$$

While expression (16) may not be obvious at first glance, its interpretation is nonetheless intuitive. Consider a shock to a single sector n, that is $\hat{\mathbf{A}} = \boldsymbol{\delta}_n$, and rewrite the Leontief inverse $\left(\mathbf{I} - \boldsymbol{\Omega}\right)^{-1}$ as $\sum_{k=0}^{\infty} \boldsymbol{\Omega}^k$. Then,

$$\mathcal{T}_{\mathbf{w}}\left(\boldsymbol{\delta}_n\right) = \underbrace{\mathbf{w}'\boldsymbol{\Omega}\left(\sum_{k=0}^{\infty} \boldsymbol{\Omega}^k\right)}_{(a)} \mathbf{diag}(\boldsymbol{\tau}) \underbrace{\left(\sum_{k=0}^{\infty} \boldsymbol{\Omega}^k\right) \boldsymbol{\delta}_n}_{(b)}.$$

To assess the contribution of each sector's delivery time, we first need to determine how frequently and intensely a sector is affected by the shock. This is represented by term (b) which quantifies the total number of walks[5] of any length k from sector n to any other intermediate sector m, weighted by the product of input shares along the path. Each of these walks is then multiplied by the corresponding τ_m (i.e., in $\mathbf{diag}(\boldsymbol{\tau})$), capturing the delivery time of the sectors reached by these paths. However, the total contribution of these sectors extends beyond this term, as additional rounds of production take place after reaching intermediate sector m. Term (a) captures these subsequent steps by representing the total (weighted) number of walks of any length k from intermediate sector m to any other final sector. This term is then multiplied by $\boldsymbol{\Omega}$ one final time, reflecting the fact that the time-to-build affects the average duration $\mathcal{T}_{\mathbf{w}}$ only after completing a full round of production.

[5] A walk of length p is any sequence of sectors $(n_0, n_1, \ldots, n_p)$ such that $\omega_{n_{k+1}n_k} > 0$ for all $k = 0, \ldots, p-1$. Edges and nodes can be repeated.

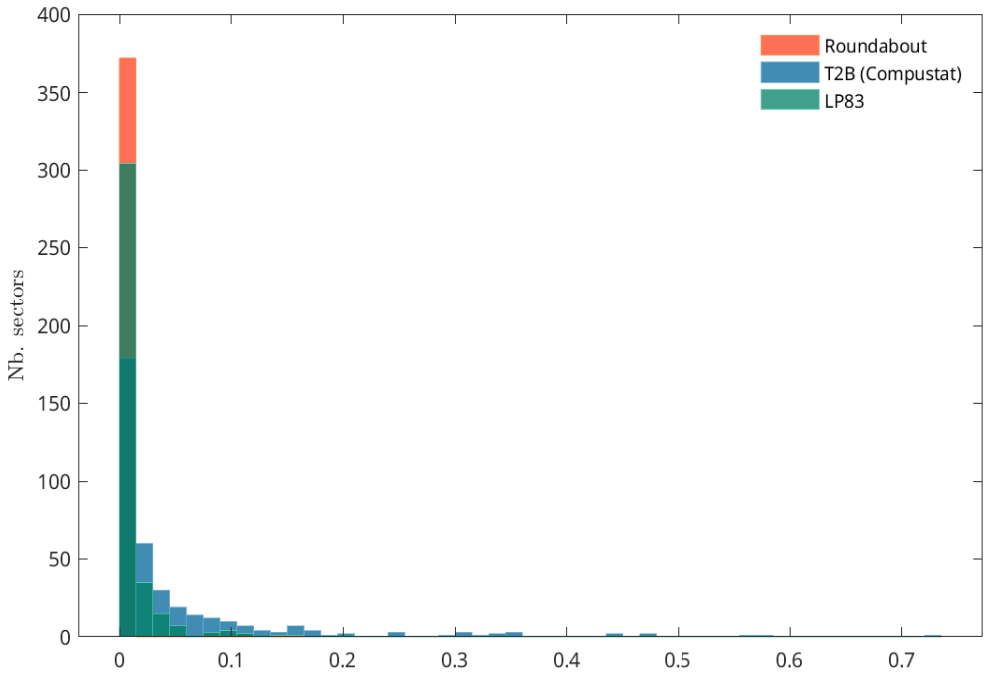

Notes: Monthly time-to-build from Compustat. We use $\mathbf{w} = \boldsymbol{\zeta}$ as weighting vector to capture the welfare relevant impact of the shock.

Figure 2: Distribution of average durations $\mathcal{T}_{\mathbf{w}}(\boldsymbol{\delta}_n)$ across sectors

Figure 2 compares the cross-sectoral distributions of the average durations $\mathcal{T}_{\mathbf{w}}(\boldsymbol{\delta}_n)$ in different models. For mere comparison, we include the roundabout economy in which the average duration statistics is strictly 0. More interestingly, the figure compares the distribution in the LP83 model with the one implied under heterogeneous time-to-build (T2B). While time-to-build is uniform and equal to 1 in the LP83, the model displays some heterogeneity in the persistence of sectoral shocks because of the structure of the production network. The overall persistence is, however, low and most sectors have an average duration close to 0. Our model exhibits significantly more propagation because certain sectors add substantial lags in production.

Figure 12 in the Appendix shows the top-20 sectors with the longest average duration. Sectoral shocks to "Electric power generation (...)" display the largest persistence with an average duration of 0.74 months (0.11 in LP83). Ignoring variation in time-to-build can thus lead to substantially underestimate the persistence of shocks.

4.2 Delay Shocks

Our model allows us to analyze the impact of *delay* shocks. We model these shocks as the delayed arrival of goods scheduled for delivery at a given point in time to a later date. We assume for

simplicity that these shocks are unanticipated.[6] Specifically, we model a T-period delay shock to sector n as the revelation at time 0 that a fraction ε of the stocks $X_{n\tau}$ for $\tau = 0, \ldots, T-1$ will only arrive T periods later. In other words, at $t = 0$ and $T \leq \tau_n/2$,

$$\begin{aligned} \hat{X}_{n\tau} &= -\varepsilon \text{ for } \tau = 0, \ldots, T-1 \\ &= +\varepsilon \text{ for } \tau = T, \ldots, 2T-1. \end{aligned}$$

Figure 3 displays the response of real GDP ($y_t = \sum_n \overline{p}_n \alpha_n y_{nt}$) in response to delay shocks of periods $T = 1$ month and 3 months to two different sectors. The top two panels show the response of delays in the sector "Nonferrous metal (...)", whose time-to-build is 3 months (Compustat). The bottom two panels display the impact of delays in the sector "Plastics material (...)", whose time-to-build is 5 months.

#331410 - Nonferrous metal smelting and refining ($\tau_n = 3$ months)

(a) 1 month (b) 3 months

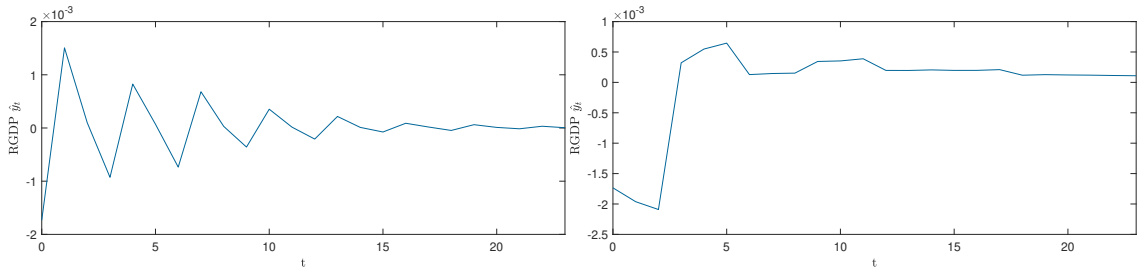

#325211 - Plastics material and resin manufacturing ($\tau_n = 5$ months)

(c) 1 month (d) 3 months

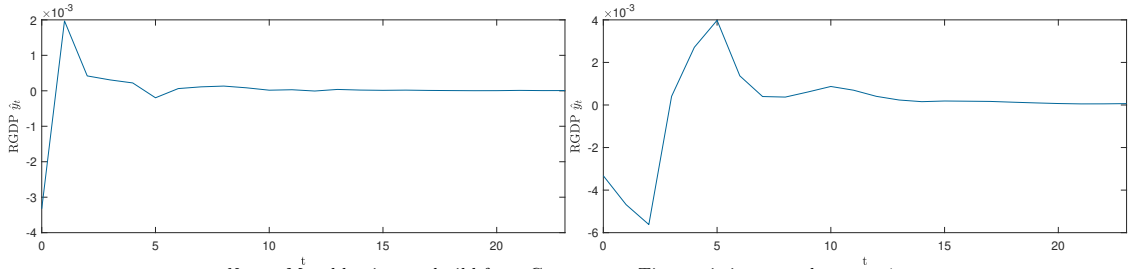

Notes: Monthly time-to-build from Compustat. Time unit is a month. $\varepsilon = -1$

Figure 3: Aggregate GDP response to delay shocks in various sectors ($T = 1$ and 3 months)

[6] This assumption is relatively innocuous in our log-linear setup in which consumption and intermediate shares are fixed and anticipation effects play no role. See, for instance, the fact that uncertainty about TFP does not affect the allocation in Proposition 1.

Several patterns can be noted from those graphs. First, as highlighted in the previous subsection, the persistence of the shocks substantially differ depending on which sector is hit. Because of its particular location in the network, delay shocks to sector #331410 ("Nonferrous metal (...)") in the top panels trigger a much more protracted response of the economy despite having a lower time-to-build. Short delay shocks can produce *oscillations*, as observed in panels (a) and (c), while longer duration delays seem to generate a smoother response. This pattern of oscillations results from two effects. It is partly due to the fact that delay shocks are by construction the combination of a negative supply shock followed by a rebound. Another deeper reason is a phenomenon of *echo* brought about by the production network, particularly present in panel (a). In that case, we observe that the initial drop in production due to a fall in inputs is repeatedly seen at regular intervals equal to the 3 months of time-to-build for that sector. This is not necessarily true for all sectors, and we explore this phenomenon further and identify its source in the next section.

4.3 Bottlenecks

In which sectors would delays significantly hinder economic activity? To answer this question, we leverage our average duration statistic to identify *bottlenecks*: sectors in which a permanent increase in time-to-build τ_n would contribute the most to the propagation of shocks.

To identify bottleneck sectors, we compute the marginal impact of a permanent delay $\partial\tau_n$ on the average duration measure $\mathcal{T}_{\mathbf{w}}$, that is, we evaluate $\partial\mathcal{T}_{\mathbf{w}}\left(\hat{\mathbf{A}}\right)/\partial\tau_n$ for a given shock $\hat{\mathbf{A}}$ and a given weighting vector $\mathbf{w}$. Proposition 3 shows that this marginal impact is the product of some appropriately weighted measures of the sector's supplier and buyer centralities.

Proposition 3. *The marginal impact of a delay shock $\partial\tau_n$ on the persistence of shock $\hat{\mathbf{A}}$ is given by the product of supplier and buyer centrality measures:*

$$\partial\mathcal{T}_{\mathbf{w}}\left(\hat{\mathbf{A}}\right)/\partial\tau_n = s_n \times b_n,$$

where $b_n = \hat{\mathbf{A}}'\left(\mathbf{I}-\boldsymbol{\Omega}'\right)^{-1}\boldsymbol{\delta}_n$ is a shock $\hat{\mathbf{A}}$-weighted measure of sector n's buyer centrality, and $s_n = \tilde{\mathbf{w}}'\left(\mathbf{I}-\boldsymbol{\Omega}\right)^{-1}\boldsymbol{\delta}_n$ is a vector $\tilde{\mathbf{w}}$-weighted measure of sector n's supplier centrality, where $\tilde{\mathbf{w}} = \boldsymbol{\Omega}'\mathbf{w}$.

Measures s_n and b_n can be interpreted as weighted centrality measures. The supplier centrality measure s_n is the more common expression. Expanding the Leontief inverse, s_n can also be expressed as

$$s_n = \tilde{\mathbf{w}}'\sum_{k=0}^{\infty}\boldsymbol{\Omega}^k\boldsymbol{\delta}_n,$$

which is sum of all walks of length k from n to any other downstream sector, weighted by the product of input shares along the path, and aggregated across sectors with vector $\tilde{\mathbf{w}}$. This weighting vector $\tilde{\mathbf{w}} = \boldsymbol{\Omega}'\mathbf{w}$ reflects both the particular weighting vector $\mathbf{w}$ chosen for the statistic $\mathcal{T}_{\mathbf{w}}$ and the fact

that a sector's time-to-build τ_n contributes to the average duration statistics after one round of the production network. As a result, if $\mathbf{w}$ is the weighting of sectors at the final stage of production, $\tilde{\mathbf{w}} = \boldsymbol{\Omega}'\mathbf{w}$ captures the implied weighting of sectors one round *before* the final stage of production.

Measure b_n can be similarly interpreted but as a *buyer* centrality measure, because it is computed using $\boldsymbol{\Omega}'$ instead of $\boldsymbol{\Omega}$ (i.e., upstream rather than downstream). Expanding the Leontief inverse, we obtain

$$b_n = \hat{\mathbf{A}}' \sum_{k=0}^{\infty} \left(\boldsymbol{\Omega}'\right)^k \boldsymbol{\delta}_n.$$

As the expression illustrates, b_n corresponds to the sum of all walks from any upstream sector m, weighted by the impact of the shock $\hat{A}_m$, to sector n. In other words, sectors with a high value for b_n are sectors that are downstream to many other sectors hit by the shock $\hat{\mathbf{A}}$.

Taking stock, Proposition 3 indicates that bottlenecks are sectors that are central to the production network, both as buyers and suppliers. This result stands in contrast to the Domar weights $\boldsymbol{\zeta}$ which reflect the importance of sectors as suppliers only.

Figure 13 in the Appendix displays the 20 largest bottleneck sectors in the U.S. economy in response to an aggregate shock. According to our definition, the most important bottlenecks are the metallurgy sectors ("Iron and steel mills (...) " and "Nonferrous metals (...)") and plastic production ("Plastics material (...)"). These bottleneck measures provide a different view of the economy than what the Domar weights suggest (Figure 11 in the Appendix).

5 Echoes and Cycles

Beyond persistence, we demonstrate in this section that the introduction of time-to-build in production networks generates rich dynamics. As demonstrated in the previous section, oscillations in response to shocks appear to be widespread once time-to-build is incorporated. In this section, we examine this phenomenon and attempt to quantify it.

5.1 Eigenvalue Spectrum

To study the emergence of oscillations, we first examine the spectrum of the dynamic system (12). For that purpose, it is useful to turn the $VAR\left(\tau_{max}\right)$ system into the following $VAR\left(1\right)$:

$$\mathbf{Y}_t = \mathbf{O}\mathbf{Y}_{t-1} + \mathbf{e}_t, \tag{17}$$

where

$$\mathbf{Y}_t = \begin{pmatrix} \hat{\mathbf{y}}_t \\ \hat{\mathbf{y}}_{t-1} \\ \vdots \\ \hat{\mathbf{y}}_{t-\tau_{max}+1} \end{pmatrix}, \mathbf{O} = \begin{pmatrix} \mathbf{\Omega}_1 & \mathbf{\Omega}_2 & \dots & & \mathbf{\Omega}_{\tau_{max}} \\ I_N & 0 & \dots & \dots & 0 \\ \ddots & I_N & \ddots & & \vdots \\ \vdots & 0 & \ddots & \ddots & \vdots \\ 0 & \dots & \ddots & I_N & 0 \end{pmatrix} \text{ and } \mathbf{e}_t = \begin{pmatrix} \hat{\mathbf{A}}_t \\ 0 \\ \vdots \\ 0 \end{pmatrix}.$$

The dynamic system governing output dynamics features oscillation when the large companion matrix $\mathbf{O}$ admits complex eigenvalues. Note that oscillations can appear in both the LP83 model and in our model with heterogeneous time-to-build, but are ruled out by construction in the roundabout economy unless the productivity process itself implies a particular pattern of serial correlations. With roundabout production and serially uncorrelated shocks, productivity disturbances are resolved within period and cannot give rise to cyclical dynamics (see equation (13) in Section 3).

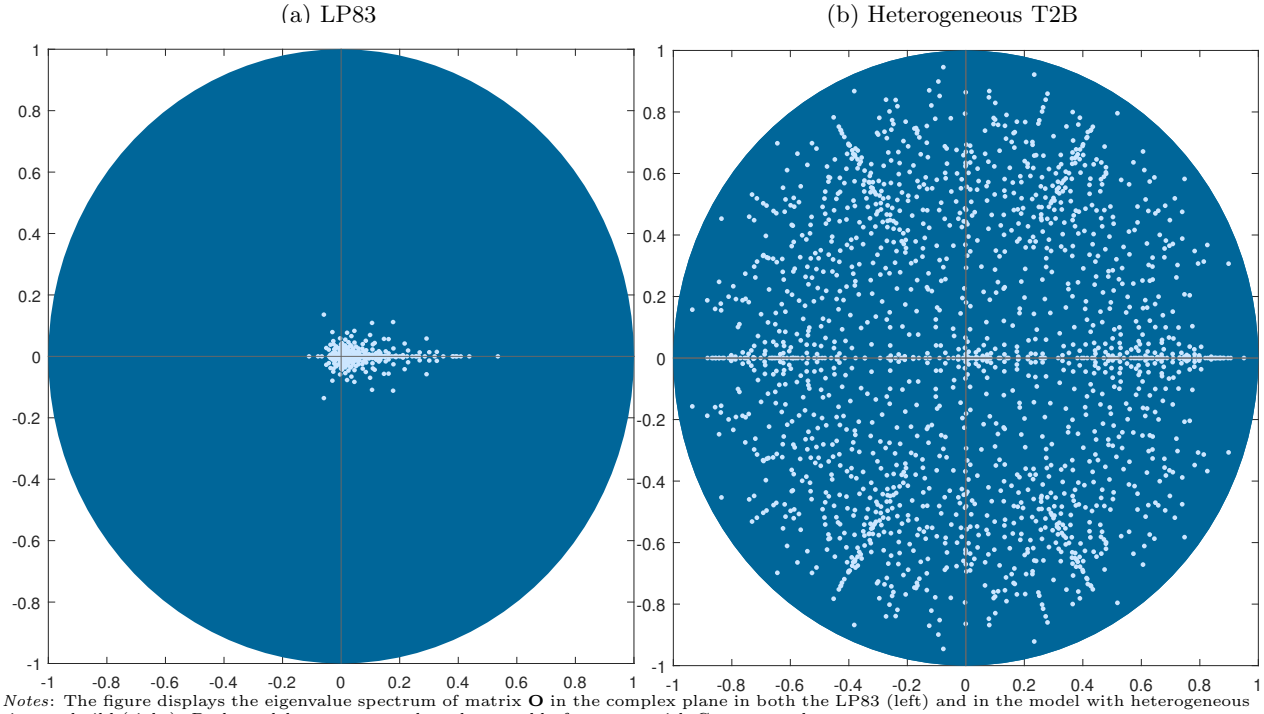

Notes: The figure displays the eigenvalue spectrum of matrix $\mathbf{O}$ in the complex plane in both the LP83 (left) and in the model with heterogeneous time-to-build (right). Both models are computed at the monthly frequency with Compustat data.

Figure 4: Eigenvalue spectrum of matrix $\mathbf{O}$

Figure 4 displays the eigenvalue spectrum of both the LP83 and our model. Several key insights can be inferred from the graph. First, because of the assumption of constant returns to scale, the rows of matrix $\mathbf{O}$ sum up to less than 1, ensuring that all the eigenvalues lie within the unit circle. Second, the comparison between the two models reveals strikingly different dynamic behaviors. In the LP83 model (left panel), eigenvalues are relatively small due to the assumption of a delivery time

uniformly set to one period. As a result, shocks dissipate quickly. The model's cyclical behavior is also minimal: most eigenvalues cluster near the real axis, with only a few exhibiting a nonzero imaginary part.

In contrast, the heterogeneous time-to-build model (right panel) presents a markedly different picture. With significantly longer delivery times (up to 2-3 years for some sectors), shocks persist over a much longer horizon, so the eigenvalues exhibit noticeably larger norms. Additionally, the spectrum reveals a richer cyclical structure with oscillations across a wide range of frequencies. The right panel of Figure 14 in the Appendix further illustrates this with a histogram of the frequencies. The model notably features peaks in angular frequencies of $\pi/3$, $2\pi/3$ and π (that is, oscillations with periods 6, 3 and 2 months). Understanding the reasons behind these remarkably different behaviors is what we turn to now.

5.2 Fourier Decomposition: a Refresher

What explains the rich dynamic behavior of the heterogeneous time-to-build model? Why are peaks at certain frequencies observed? Can the structure of the production network account for these patterns?

To address these questions, we turn to the model's Fourier spectrum. Like the eigenvalue spectrum, Fourier analysis offers a decomposition of the model's dynamics into cyclical components using sines and cosines. However, Fourier analysis bypasses the need to explicitly compute the model's eigenvalues—a task that cannot be done analytically for a general input-output matrix.

Following Hamilton (2020), any discrete-time 0-mean stationary process y_t can be represented as

$$y_t = \int_{-\pi}^{\pi} \delta(\omega)\, e^{i\omega t} d\omega,$$

where $E[\delta(\omega)] = 0$ and $E[\delta(\omega)\,\delta(\omega')] = 0$ for $\omega \neq \omega'$. Function $\delta(\omega)$ is a (complex-valued) random variable that we refer to as the *discrete time Fourier transform* (DTFT) of process y_t. It can be derived from the expression

$$\delta(\omega) = \frac{1}{2\pi} \sum_{t=-\infty}^{\infty} y_t e^{-i\omega t}.$$

Of particular interest is the *spectral density function*, defined as $f(\omega) = E\left[\delta(\omega)\,\overline{\delta(\omega)}\right]$, which captures how much a certain process y_t loads onto a certain frequency ω. Lastly, it is also useful to introduce the *autocorrelation function* (ACF) $\gamma_k = E[y_t y_{t-k}]$ for $k = -\infty, \ldots, \infty$. A key property that we use extensively is that the spectral density f is the DTFT of the ACF, i.e.,

$$f(\omega) = \frac{1}{2\pi} \sum_{k=-\infty}^{\infty} \gamma_k e^{-i\omega k}. \tag{18}$$

To compute the Fourier spectrum of a given sector n, we calculate the sector's ACF $\gamma_k(n) = E[\hat{y}_{nt}\hat{y}_{n,t-k}]$. This can be done analytically in our context because the economy is governed by the simple VAR(1) process (17). According to Lütkepohl (2005), the *autocovariance matrix function* (ACMF) $\mathbf{\Gamma}_k = E\left[\mathbf{Y}_t\mathbf{Y}'_{t-k}\right]$ is given by

$$\mathbf{\Gamma}_0 = \sum_{k=0}^{\infty} \mathbf{O}^k \mathbf{\Sigma} \left(\mathbf{O}'\right)^k \text{ and } \mathbf{\Gamma}_k = \mathbf{O}^k \mathbf{\Gamma}_0,\ k > 0, \tag{19}$$

where $\mathbf{\Sigma} = E[\mathbf{e}_t\mathbf{e}'_t]$ is the variance-covariance matrix of the productivity shocks.

5.3 Network Cycles

Although equation (19) offers an expression that can be readily used to compute the autocorrelation function and the Fourier spectrum for any sector in the economy, the expression remains relatively abstract and does not provide deeper insights into how the structure of the production network shape the economy's cyclical behavior.

Rather than pursuing this route, we note that any serial correlation for a given sector i must arise from the existence of *cycles* in the network. That is, the existence of walks from sector i to itself, either *directed* or *undirected*. Figure 5 illustrates these two cases. Panel (a) depicts the hypothetical existence of a *directed* cycle of length p from sector n to itself, i.e., a sequence of nodes $(n = n_0, n_1, \ldots, n_{p-1}, n_0)$ connected by arrows that indicate nonzero flows of intermediate inputs between the sectors. Such a cycle naturally leads to serial correlation as shocks that hit sector n travel along the path and reappear $\sum_{k=0}^{p-1} \tau_{n_k}$ periods later. Serial correlation can also

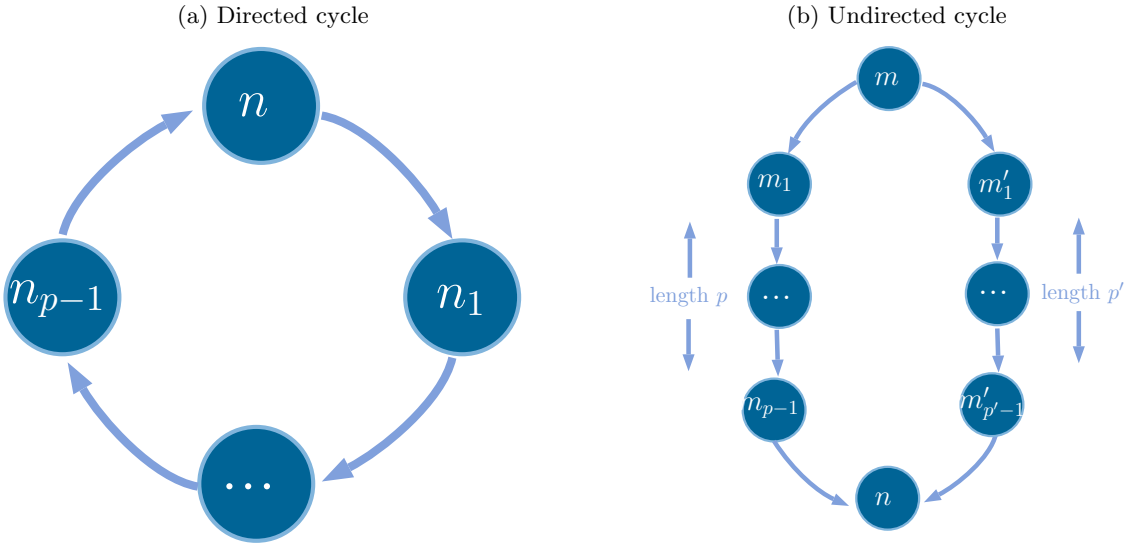

Figure 5: Serial Correlation and Cycles

arise in the presence of *undirected* cycles, depicted in panel (b). The graph describes a hypothetical

situation in which sector m is connected to sector n by two paths: a walk of length p on the left ($m = m_0, m_1, \ldots, m_p = n$) and a walk of length p' on the right $\left(m = m_0, m'_1, \ldots, m'_{p'} = n\right)$. The arrows indicate the flow of intermediate goods from sector m to sector n along the two paths and point towards opposite directions when reaching sector i. In that sense, the union of the two paths does not form a proper cycle in the directed graph associated to the production network, but it does in the associated undirected graph (i.e., ignoring the arrows' directions). Such an undirected cycles can create serial correlation in sector n: shocks that hit sector m travel along the two paths and appear $T = \sum_{k=0}^{p-1} \tau_{m_k}$ periods later in sector n from the path on the left and $T' = \sum_{k=0}^{p'-1} \tau_{m'_k}$ periods later from the path on the right. In other words, sector n can display serial correlation at the lag $|T - T'|$.

We focus our analysis on the directed cycles. We will show later that these directed cycles account for virtually all the ACF and Fourier spectrum of the economy. For a given directed cycle $\varsigma = (n_0, n_1, \ldots, n_{p-1}, n_p = n_0)$, we define the cycle's length $l(\varsigma) = p$ the number of edges crossed, its duration $\tau(\varsigma) = \sum_{k=0}^{p-1} \tau_{n_k}$ and weight $w(\varsigma) = \prod_{k=0}^{p-1} \omega_{n_{k+1} n_k}$. In the case of i.i.d. productivity shocks, the ACF of a given sector consists of positive terms, among which we can isolate the contribution of a specific cycle. Figure 15 in the Appendix illustrates the propagation of shocks through a cycle ς. Shocks reaching sector n_0 at time t—this includes $\hat{A}_{n_0 t}$ and other shocks originated upstream in the past—travel along the cycle and appear τ_{n_0} periods later in sector n_1, scaled by $\omega_{n_1 n_0}$. The process continues with shocks propagating to sector n_2 after an additional τ_{n_1} periods, multiplied by $\omega_{n_2 n_1}$ and so forth. Ultimately, the shocks return to sector n_0 after a total number of periods $\tau(\varsigma)$, scaled by the weight $w(\varsigma)$. From this, we derive a lower bound[7] for the contribution of cycle ς to the ACF and to the Fourier spectrum of sector i_0, formalized in Proposition 4.

Proposition 4. *If productivity shocks are i.i.d., a $p-$cycle $\varsigma = (n_0, n_1, \ldots, n_{p-1}, n_p = n_0)$ contributes (at least) to the ACF of sector n_0:*

$$\gamma_{k\tau(\varsigma)}(n_0) = w(\varsigma)^{|k|} \sigma^2(\hat{y}_{n_0 t}) \tag{20}$$

for $k \in \mathbb{N}$ and to the Fourier spectrum

$$f_{n_0}(\omega) = \frac{\sigma^2(\hat{y}_{n_0 t})}{2\pi} \frac{1 - w(\varsigma)^2}{1 + w(\varsigma)^2 - 2w(\varsigma) cos(\omega\tau(\varsigma))}, \tag{21}$$

where $\sigma(\hat{y}_{n_0,t})$ is the standard deviation of $\hat{y}_{n_0 t}$, $\tau(\varsigma)$ is the duration and $w(\varsigma)$ the weight of cycle ς.

[7] This lower bound represents the contribution of cycle ς in isolation of the rest of the network. If cycle ς intersects with other cycles, additional positive terms may appear in the ACF, meaning that (20) provides only a lower estimate of the total contribution of cycle ς. We show later that this lower bound accounts for virtually all the serial correlation using the U.S. input-output matrix from the BEA.

Proposition 4 demonstrates that directed cycles imply a particular lagged structure in the ACF, characterized by peaks at multiples of the cycle's duration τ and a dampening effect determined by the weight w. Consequently, this lag structure in the ACF gives rise to distinct peaks in the frequency domain. Figure 6 provides an example with the Fourier spectrum (21) of a cycle of duration $\tau = 3$ with varying weights ($w = 0.25$, 0.5, and 0.75). As shown, a network cycle of length 3 produces peaks at corresponding angular frequencies—multiples of $2\pi/3$. The spectrum is rather diffuse for low values of the weight but the peaks become increasingly pronounced as the weight grows. In essence, the network's topology determines the Fourier spectrum of a sector, while the Fourier spectrum, in turn, reveals the underlying cyclical composition of the network.

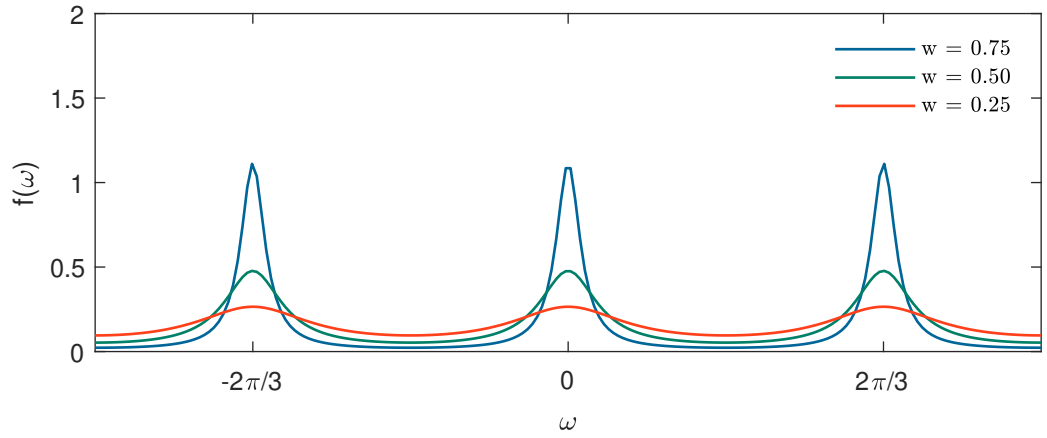

Figure 6: Spectrum of a cycle of duration $\tau = 3$ for different weights

5.4 Counting Cycles

Having established their significance in shaping the economy's cyclical behavior, we parse the network in an attempt to identify its cycles, recording their durations and weights. Detecting cycles in a graph is a highly combinatorial problem, making brute-force enumeration feasible only for short cycles (i.e., those involving 2 or 3 nodes, given standard computing power and the BEA's input-output network). For longer cycles, we employ a population of crawlers that travel the network at random, recording cycles whenever they are encountered. While this approach does not guarantee a complete enumeration of all cycles, it proves sufficient for our purposes, as we will demonstrate later.

Table 1 presents the highest-weight cycles in the network. Our network exploration reveals an abundance of self-cycles with substantial weights.[8] The number of cycles of length greater than 2 is even larger, but they tend to carry lower weights.

[8]This reflects the fact that the diagonal in the U.S. input-output matrix is large. We must remain cautious interpreting those as actual cycles in production because they can be an artifact of aggregation. Figure 16 in the appendix provides an example of how aggregation can lead to the emergence of false self-loops.

Weight	Duration	Sectors
Length 1		
0.43	3	#331410 – Nonferrous metal (except alum.) smelting and refining
0.41	6	#1121A0 – Beef cattle ranching and farming (...)
0.39	6	#312140 – Distilleries
Length ≥2		
0.03	3	#325110 – Petrochemical manufacturing
		#325190 – Other basic organic chemical manufacturing
0.01	14	#336310 – Motor vehicle gasoline engine and engine parts (...)
		#333618 – Other engine equipment manufacturing
0.01	8	#322130 – Paperboard mills
		#322210 – Paperboard container manufacturing

Notes: Input-output network from the BEA and time-to-build from Compustat. Duration in months.

Table 1: Top-3 cycles by weight and length

Figure 7 presents various statistics regarding the cycles that we identify in the U.S. input-output matrix. Panel (a) presents the number of cycles as a function of their length. The exact counts of cycles of lengths 1 (self-cycles) and 2 are indicated in orange, while cycles detected using crawlers appear in blue. Since our search method is not exhaustive for cycles of length greater than 2, their count is significantly lower—though this has minimal impact, as these cycles carry small weights and contribute little to the overall Fourier spectrum, as we demonstrate later. Panel (b) shows the same distribution but weighted. In the LP83 model, where delivery times are restricted to 1, cycle lengths and durations coincide. The figure reveals that cycles of length 1 dominate, while longer cycles are nearly negligible, explaining the LP83 model's lack of cyclical behavior, as evidenced in its eigenvalue spectrum (4). Panel (c) and (d) display the unweighted and weighted distributions of cycle durations, respectively. The results confirm the presence of a diverse range of cycles of varying durations, supporting the rich eigenvalue spectrum observed in the model with heterogeneous time-to-build. Notably, panel (d) highlights distinct peaks for cycles of duration 3 and 6 months (and, to a lesser extent, 2 months), aligning with the frequency peaks seen in the eigenvalue spectrum of Figure 14 in the appendix.

These findings support the crucial role of network cycles in shaping the economy's cyclical dynamics.

5.5 From Network Cycles to Business Cycles

Having identified the primary directed cycles within the production network, we now assess to what extent those cycles can account for the Fourier spectrum of each sector. To do this, we enumerate all the cycles a sector belongs to and sum up their contributions, captured by equation (20), to the

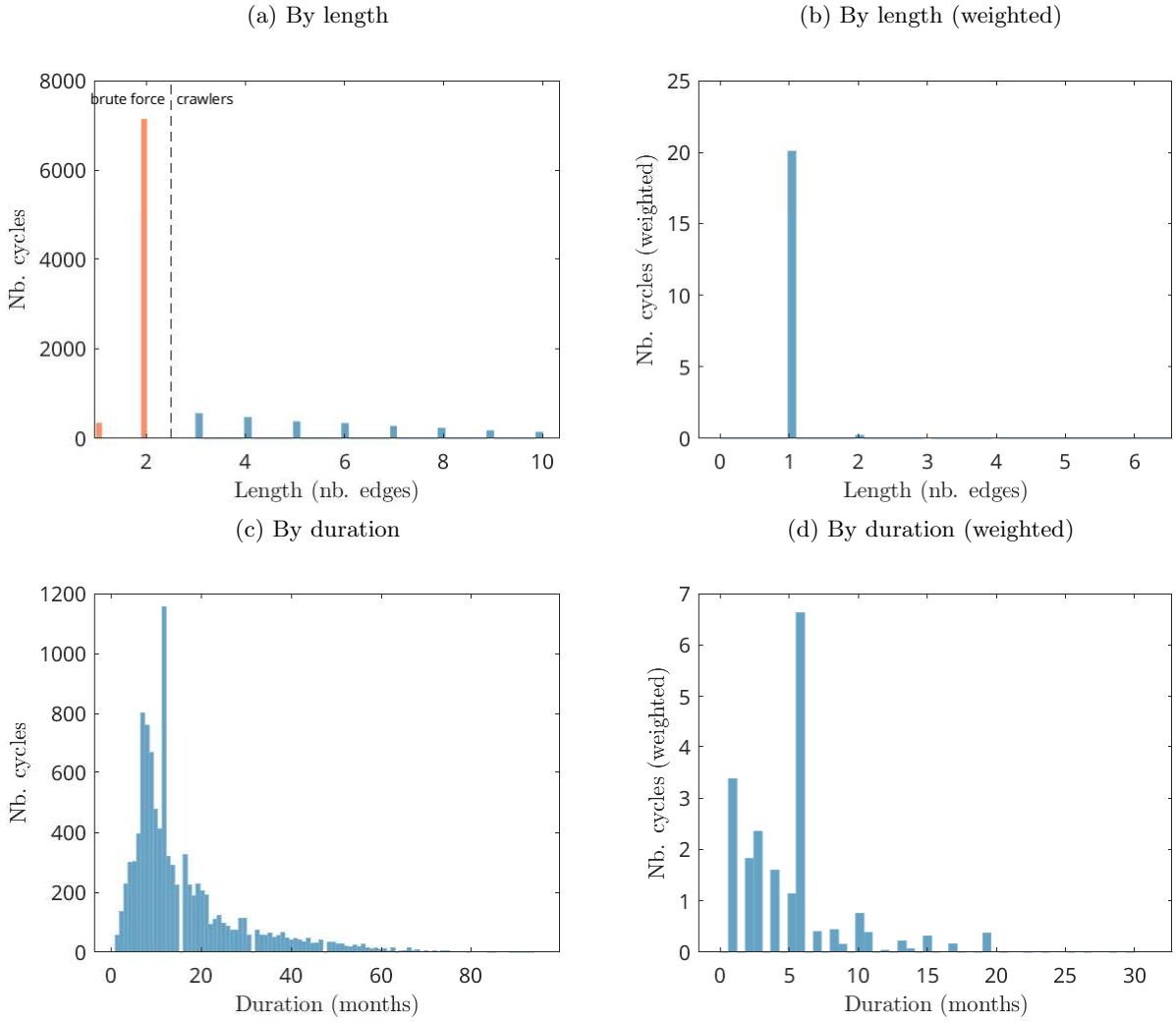

Notes: Input-output network from the BEA and time-to-build from Compustat. This figure was produced by brute force for cycles of length (number of edges crossed) ≤ 2 and 250 crawlers for higher lengths. Panel (c) shows the distribution of the cycle durations $\tau(\varsigma)$ using $w(\varsigma)$ as weights.

Figure 7: Network cycle statistics

sector's ACF. Because our search of cycles is not exhaustive and that equation (20) is only a lower bound on a cycle's contribution, we anticipate explaining only a fraction of the full ACF, which we compute using (19).

Surprisingly, the directed cycles account for nearly *the entire ACF*: we obtain an astonishing R^2 of 0.9996 across sectors and over a 5-year horizon. Figure 8 provides two illustrative examples that highlight the explanatory power of the directed cycles. The graph compares over multiple lags the full ACF to the one derived solely from the directed cycles. Panel (a) depicts sector #331410 ("Nonferrous metal (...)"), which is part of the largest self-cycle we identify. The ACF exhibits peaks at 3-month intervals, directly reflecting the main cycle's duration. Panel (b) presents another example with sector #1121A0 ("Beef cattle ranching and farming (...)"). This sector belongs to the second most important cycle reported in Table 1 with 0.41 and duration 6 month. As predicted

by the cycle, the ACF displays declining peaks at regular intervals of 6 months.

(a) Nonferrous metal

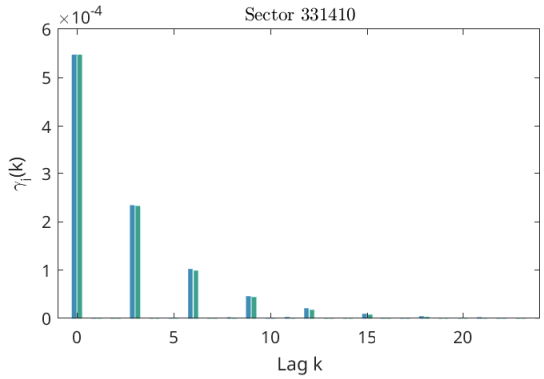

(b) Beef cattle ranching and farming (...)

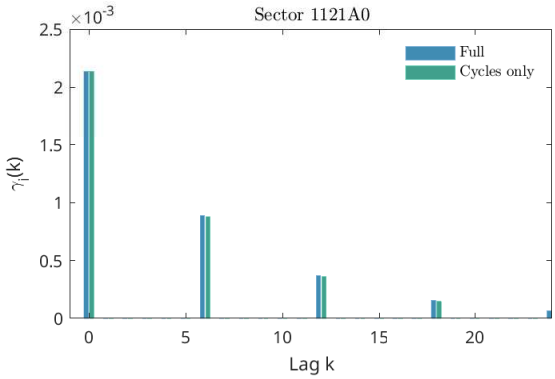

Figure 8: Examples of ACF: full vs. directed cycle-only

Due to the equivalence between the ACF and the Fourier spectrum, the production network's directed cycles also determine the model-implied Fourier decomposition of the economy's sectors. Figure 9 illustrates the Fourier spectrum for the two previously analyzed sectors, presented both in terms of angular frequency (top panels) and oscillation period (bottom panels). In both cases, the duration of the dominant cycles (3 and 6 months respectively) are prominently reflected in the Fourier spectrum. We note further that panel (b) exhibits peaks located at integer divisors of the primary cycle's 6-months period (i.e., at 2 and 3 months, corresponding to angular frequencies $\omega = \pi$ or $2\pi/3$). This property is a fundamental characteristic of the system we study, arising from the specific structure of the ACF (20), and captured by the Fourier spectrum (21).[9]

6 Sectoral Comovements and Aggregation

Our analysis has so far primarily examined the dynamics of individual sectors. In this section, we broaden our scope to explore how heterogeneous time-to-build gives rise to complex cross-sectoral comovements. We examine afterwards the implications of both sector-specific and cross-sectoral dynamics for GDP fluctuations.

6.1 Multi-sector IRFs

We begin our analysis of dynamic sectoral comovements by examining multi-sector impulse responses (IRFs) to sectoral shocks. Figure 17 in the appendix displays the response over time of all

[9] In the presence of a cycle of duration τ, the ACF is 0 everywhere except at multiples of τ. Computing the Fourier spectrum of the sectors involved in the cycle is thus equivalent to calculating the Fourier transform of a signal sampled at discrete τ intervals, which cannot distinguish between the base frequency τ and its harmonics (i.e., integer multiples).

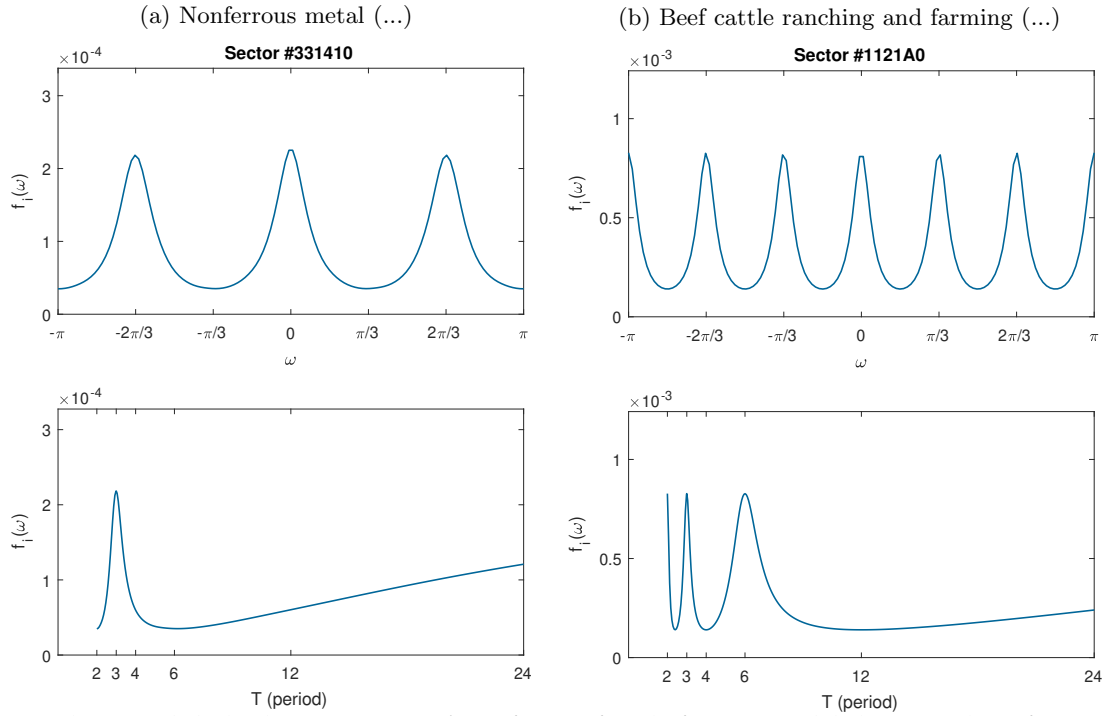

Notes: The top panels display the Fourier spectrum f_n as a function of angular frequency ω and the bottom panels as a function of the period $T = 2\pi/\omega$.

Figure 9: Examples of Fourier spectra

sectors to a positive 1% productivity shock to sector #334110 ("Petroleum Refineries"). The magnitude of the impact is indicated by the size and darkness of the dots. The right panel summarizes the broad cross-sectoral impact of the shock by showing a weighted histogram of the cumulative sectoral response. The bottom panel displays the response of real GDP in percentage terms, which we define as total value added in constant steady-state prices: $y_t = \sum_n \overline{p}_n \alpha_n y_{nt}$.

Sector #334110 has a high Domar weight and is a key supplier to many industries. This is reflected in the histogram's widespread impact across the economy. Following the initial shock at $t = 0$, direct customers of sector #334110 experience effects after a two-month delivery lag. The shock then propagates further downstream, affecting subsequent buyers in the supply chain. While sector #334110 is not itself part of an important cycle, some of its downstream buyers are. As the shock spreads throughout the economy, it triggers cyclical fluctuations in downstream sectors that belong to cycles. Notably, we observe a recurring 6-month cycle in multiple sectors, which also manifests itself in GDP fluctuations at regular intervals ($t = 2, 8, 14, \ldots$).

Figure 18, also in the appendix, provides another example, this time focusing on a sector that belongs to a large cycle: sector #331410 ("Nonferrous metal (...)"). As previously noted, this sector belongs to a self-cycle with a 3-month duration. As expected, a distinct 3-month cyclical pattern emerges—not only in sector #331410 but also in all its immediate buyers. The pattern is clearly visible in GDP ($t = 3, 6, 9, \ldots$). This observation highlights an important insight: the

cyclical patterns produced by the network's cycles are not only observed within the directly involved sectors but also in the downstream sectors, ultimately shaping aggregate economic dynamics.

These examples illustrate the complex dynamic comovements that arise as a result of input-output linkages and time-to-build. These dynamics confirm the importance of the network's cycles but also suggest an important role for the particular structure of the input-output relationships that connect those cycles to their downstream partners.

6.2 Dominant walks

How does the structure of the network shape the comovements across sectors?

Equation (19) can be used to compute the correlation across sectors at any lag. But as we previously argued, this expression provides little insight into the role of the network structure behind those dynamic comovements.

Consider instead the MA representation of sector n's output:

$$\hat{y}_{nt} = \hat{A}_{nt} + \sum_m \omega_{nm} \hat{y}_{m,t-\tau_m} = \hat{A}_{nt} + \sum_m \omega_{nm} \hat{A}_{m,t-\tau_m} + \sum_m \sum_l \omega_{nm}\omega_{ml} \hat{A}_{l,t-\tau_m-\tau_l} + \dots \tag{22}$$

Extending the notation we previously introduced for cycles, define for a walk $\varsigma = (n_0, \dots, n_p)$ its length $l(\varsigma) = p$, its duration $\tau(\varsigma) = \sum_{k=0}^{p-1} \tau_{n_k}$ and weight $w(\varsigma) = \prod_{k=0}^{p-1} \omega_{n_{k+1}n_k}$. Let us also denote $\mathcal{P}_\tau(n,m)$ the set of all the walks of duration τ from sector n to m in the production network and $\mathcal{P}(n,m) = \cup_{\tau \geq 0} \mathcal{P}_\tau(n,m)$. Then, equation (22) can be rewritten as

$$\hat{y}_{nt} = \hat{A}_{nt} + \sum_m \sum_{\varsigma \in \mathcal{P}(m,n)} w(\varsigma) \hat{A}_{m,t-\tau(\varsigma)}. \tag{23}$$

Using this MA notation and maintaining the assumption of $i.i.d$ shocks, it now becomes possible to write the contemporaneous correlation across sectors as

$$E[\hat{y}_{nt}\hat{y}_{mt}] = [\mathbf{\Gamma}_0]_{nm} = \sum_{\tau=0}^{\infty} \sum_{k=1}^{N} \sum_{\substack{\varsigma_{k\to n} \in \mathcal{P}_\tau(k,n) \\ \varsigma_{k\to m} \in \mathcal{P}_\tau(k,m)}} w(\varsigma_{k\to n}) w(\varsigma_{k\to m}) \sigma^2\left(\hat{A}_k\right). \tag{24}$$

In other words, equation (24) shows that two sectors n and m can be correlated at time t if a shock to another sector k at time $t-\tau$ is propagated through a walk from k to n and a walk from k to m of equal lengths τ.

We can similarly compute the lagged cross-sectoral correlation

$$E\left[\hat{y}_{nt}\hat{y}_{mt-l}\right] = \left[\boldsymbol{\Gamma_l}\right]_{nm} = \sum_{\tau=0}^{\infty}\sum_{k=1}^{N} \sum_{\substack{\varsigma_{k\to n} \in \mathcal{P}_{\tau+l}(k,n) \\ \varsigma_{k\to m} \in \mathcal{P}_{\tau}(k,m)}} w\left(\varsigma_{k\to n}\right) w\left(\varsigma_{k\to m}\right) \sigma^2\left(\hat{A}_k\right). \tag{25}$$

Intuitively, sector n at time t can be correlated with sector m at time $t-l$ if a shock to another sector k at time $t-(\tau+l)$ is propagated through a walk from k to n of length $\tau+l$ and a walk from k to m of length τ.

Echoing our decomposition of sectoral dynamics into *dominant cycles*, equations (24) and (25) show that the comovement between any two sectors at any lag can be decomposed as the sum of *dominant walks*.

6.3 Aggregation

After studying the dynamics of individual sectors and cross-sectoral comovements, we turn to the implications of input-output linkages and heterogenous time-to-build on GDP.

We consider aggregate real value added in constant steady-state prices $y_t = \sum \alpha_n \overline{p}_n y_{nt}$. In log deviations from steady state, GDP is given by $\hat{y}_t = \sum_{n=1}^{N} \mu_n \hat{y}_{nt}$ where $\mu_n = \alpha_n \overline{p}_n \overline{y}_n / \sum_m \alpha_m \overline{p}_m \overline{y}_m$. To evaluate its Fourier spectrum, we proceed as before by computing the ACF:

$$E\left[\hat{y}_t \hat{y}_{t-k}\right] = E\left[\boldsymbol{\mu}' \hat{\mathbf{y}}_t \hat{\mathbf{y}}_{t-k} \boldsymbol{\mu}\right] = \boldsymbol{\mu}' \boldsymbol{\Gamma}_k \boldsymbol{\mu}, \tag{26}$$

where $\boldsymbol{\Gamma}_k$ is the ACMF of the entire vector of sectoral outputs, as defined in (19). Expression (26) highlights the dependence of the GDP's autocorrelation function on the ACMF of the entire system. Using this expression, we may now evaluate the density spectrum of GDP.

Proposition 5. *The Fourier spectrum of aggregate real GDP is given by*

$$f_y(\omega) = \sum_{n=1}^{N} \mu_n^2 f_n(\omega) + \frac{1}{2\pi} \sum_{n\neq m} \sum_{k=-\infty}^{\infty} \mu_n \mu_m \left[\boldsymbol{\Gamma}_k\right]_{nm} e^{-i\omega k}. \tag{27}$$

Proposition 5 shows that the spectrum of GDP can be decomposed into two terms. The first key insight is that sectoral cycles—shaped by the network topology and the existence of cycles—survive aggregation. The first term $\left(\sum_{n=1}^{N} \mu_n^2 f_n(\omega)\right)$ represents a weighted sum of each sector's individual density spectrum, which, as previously discussed, is mainly driven by the *dominant cycles* of the production network. The second term $\left(\sum_{n\neq m} \sum_{k=-\infty}^{\infty} \mu_n \mu_m \left[\boldsymbol{\Gamma}_k\right]_{nm} e^{-i\omega k}\right)$ emphasizes the role of cross-sectoral comovements in shaping GDP fluctuations. Since GDP is a weighted sum of sectoral outputs, comovements across sectors are a source of serial correlation in GDP. As noted in the

previous section, this component can also be decomposed into the network's *dominant walks* across sectors.

To illustrate how these various components shape the dynamics of GDP, Figure 10 displays its full model-implied spectrum (in black), along with the contribution of the each sector's individual spectrum (in blue).

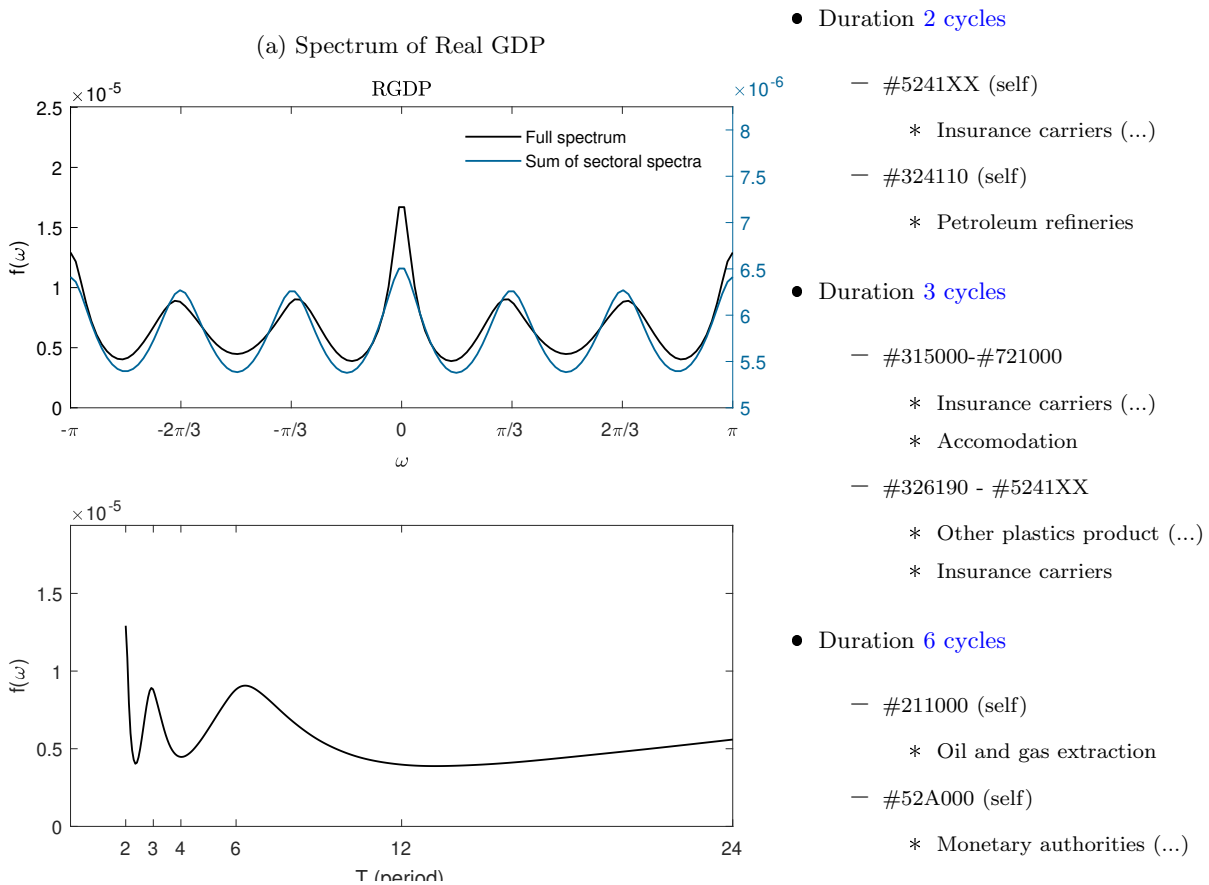

Notes: Input-output network from the BEA and time-to-build from Compustat. The left vertical axis in the top left panel corresponds to the full spectrum and the right vertical axis to the one implied by the sectoral spectra. The top left panel shows the spectrum in terms of angular frequency, the lower left panel shows the spectrum in period $T = 2\pi/\omega$.

Figure 10: Spectrum of Real GDP

The top left panel shows that the sum of each sector's spectrum aligns closely with the full spectrum when the right axis is appropriately scaled. We find that this component accounts for approximately one half of the full spectrum, with the remaining variation explained by the comovement term. Notably, the frequency peaks are accurately identified, allowing to trace them back to the network's cycles. Consistent with our earlier findings on the eigenvalue spectrum (Figure 14 in the appendix), we observe distinct peaks corresponding to cycles of durations 2, 3 and 6 months. The right panel indicates the network cycles that contribute the most to the observed peaks at those durations according to our decomposition.

In conclusion, heterogeneous time-to-build generates complex dynamics in production network economies, both at the sectoral and aggregate levels. Our results underscore the critical role of network topology—particularly its dominant cycles and paths—in shaping aggregate dynamics.

7 Quantitative Application

Under construction.

8 Conclusion

In this paper, we examine how heterogeneous time-to-build affects sectoral and aggregate dynamics in a production network economy. We show that time-to-build significantly contributes to the persistence of shocks, with highly heterogeneous effects across sectors. We further analyze the impact of delay shocks across sectors and characterize bottlenecks—sectors in which delays substantially hinder economic activity. Our results show that bottlenecks can be characterized by the product of the sector's buyer and supplier centralities.

The introduction of heterogeneous time-to-build generates complex sectoral and aggregate dynamics. We demonstrate that endogenous fluctuations arise due to cycles in the network (both directed and undirected). Our findings show that the Fourier spectrum of a sector's output can be predicted by the weights and durations of the network cycles it belongs to. Sectoral comovements are similarly intricate and can be decomposed into the network's dominant paths. Finally, we establish that these sectoral fluctuations survive in the aggregate and characterize the Fourier spectrum of aggregate GDP as a function of the production network's dominant cycles and walks.

Our framework is intentionally simple and frictionless. In future research, we plan to investigate how departures from our baseline log-linear model affect the propagation of shocks. We would like to consider in particular how the introduction of inventories could further dampen or amplify economic fluctuations. Another promising avenue would be to investigate how time-to-build affects the timing of price adjustments in models with price rigidities.

References

Acemoglu, D., V. M. Carvalho, A. Ozdaglar, and A. Tahbaz-Salehi (2012). The network origins of aggregate fluctuations. *Econometrica 80*(5), 1977–2016.

Acemoglu, D., A. Ozdaglar, and A. Tahbaz-Salehi (2017, jan). Microeconomic origins of macroeconomic tail risks. *American Economic Review 107*(1), 54–108.

Alessandria, G., S. Y. Khan, A. Khederlarian, C. Mix, and K. J. Ruhl (2023). The aggregate effects

of global and local supply chain disruptions: 2020–2022. *Journal of international Economics 146*, 103788.

Baqaee, D. R. and E. Farhi (2019a). The macroeconomic impact of microeconomic shocks: Beyond hulten's theorem. *Econometrica 87*(4), 1155–1203.

Baqaee, D. R. and E. Farhi (2019b, sep). Productivity and misallocation in general equilibrium. *Quarterly Journal of Economics 135*(1), 105–163.

Benhabib, J. and K. Nishimura (1979). The hopf bifurcation and the existence and stability of closed orbits in multisector models of optimal economic growth. *Journal of Economic Theory 21*(3), 421–444.

Carvalho, V. M. and M. Reischer (2021). Pathways to persistence. Working paper.

Djankov, S., C. Freund, and C. S. Pham (2010). Trading on time. *The review of Economics and Statistics 92*(1), 166–173.

Hamilton, J. D. (2020). *Time series analysis*. Princeton university press.

Hulten, C. R. (1978, oct). Growth accounting with intermediate inputs. *Review of Economic Studies 45*(3), 511–518.

Hummels, D. L. and G. Schaur (2013). Time as a trade barrier. *American Economic Review 103*(7), 2935–2959.

Jones, C. I. (2011, apr). Intermediate goods and weak links in the theory of economic development. *American Economic Journal: Macroeconomics 3*(2), 1–28.

Kydland, F. E. and E. C. Prescott (1982, November). Time to build and aggregate fluctuations. *Econometrica 50*(6), 1345.

Liu, E. (2019, aug). Industrial policies in production networks. *Quarterly Journal of Economics 134*(4), 1883–1948.

Liu, E. and A. Tsyvinski (2024, 01). A dynamic model of input output networks. *The Review of Economic Studies 91*(6), 3608–3644.

Long, J. B. J. and C. I. Plosser (1983). Real business cycles. *Journal of political Economy 91*(1), 39–69.

Lütkepohl, H. (2005). *New introduction to multiple time series analysis*. Springer.

A Additional Figures

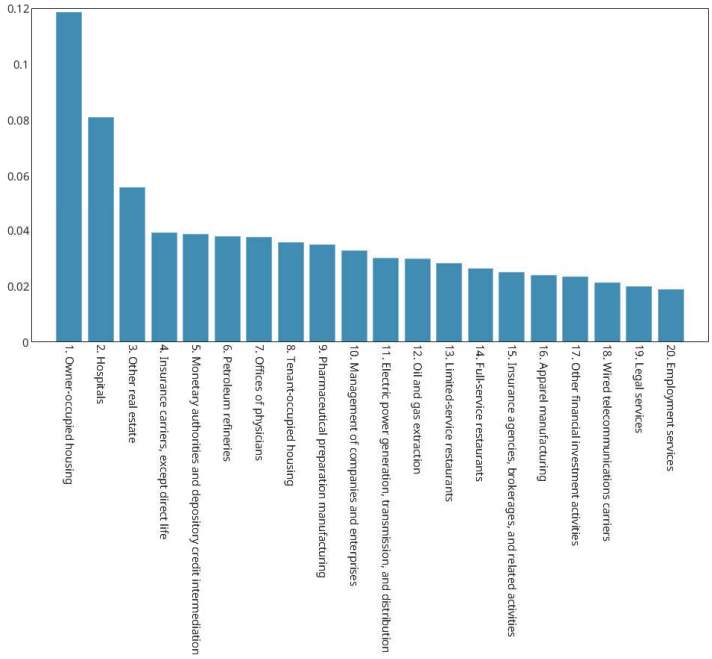

Notes: Monthly time-to-build from Compustat. Consumption spending shares from the BEA, $\beta = 0.96^{\frac{1}{12}}$.

Figure 11: Top-20 Domar weights $\boldsymbol{\zeta}$

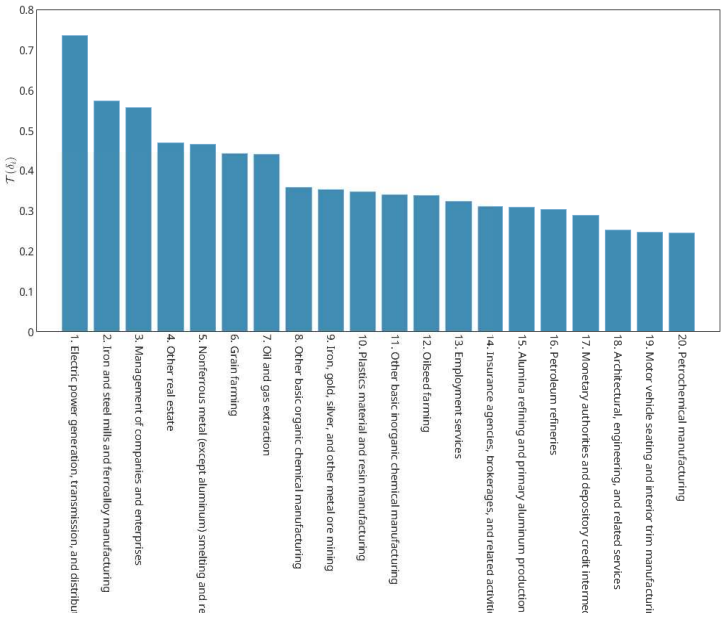

Notes: Monthly time-to-build from Compustat. We use $\mathbf{w} = \boldsymbol{\zeta}$ as weighting vector.

Figure 12: Top-20 sectors with largest average duration $\mathcal{T}_{\mathbf{w}}(\boldsymbol{\delta}_i)$ (Compustat)

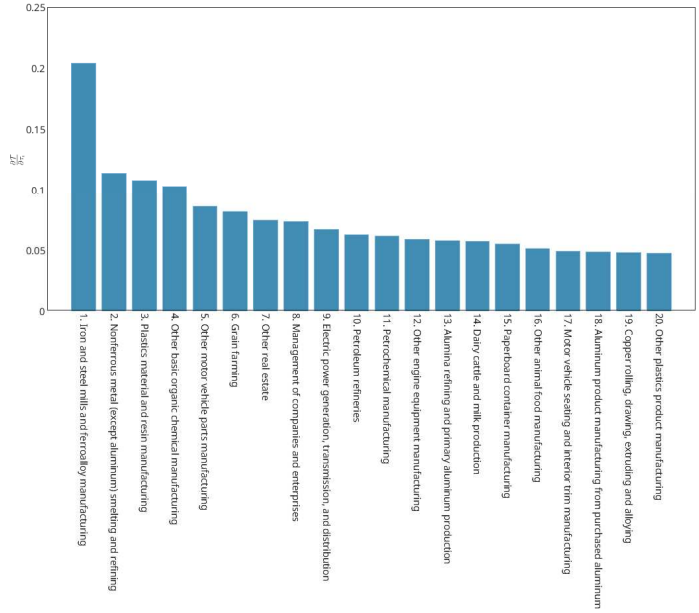

Notes: Monthly time-to-build from Compustat. We use weighting vector $\mathbf{w} = \boldsymbol{\zeta}$ and aggregate shock $\hat{\mathbf{A}} = \mathbf{1}$.

Figure 13: Top-20 largest bottleneck sectors to aggregate shocks

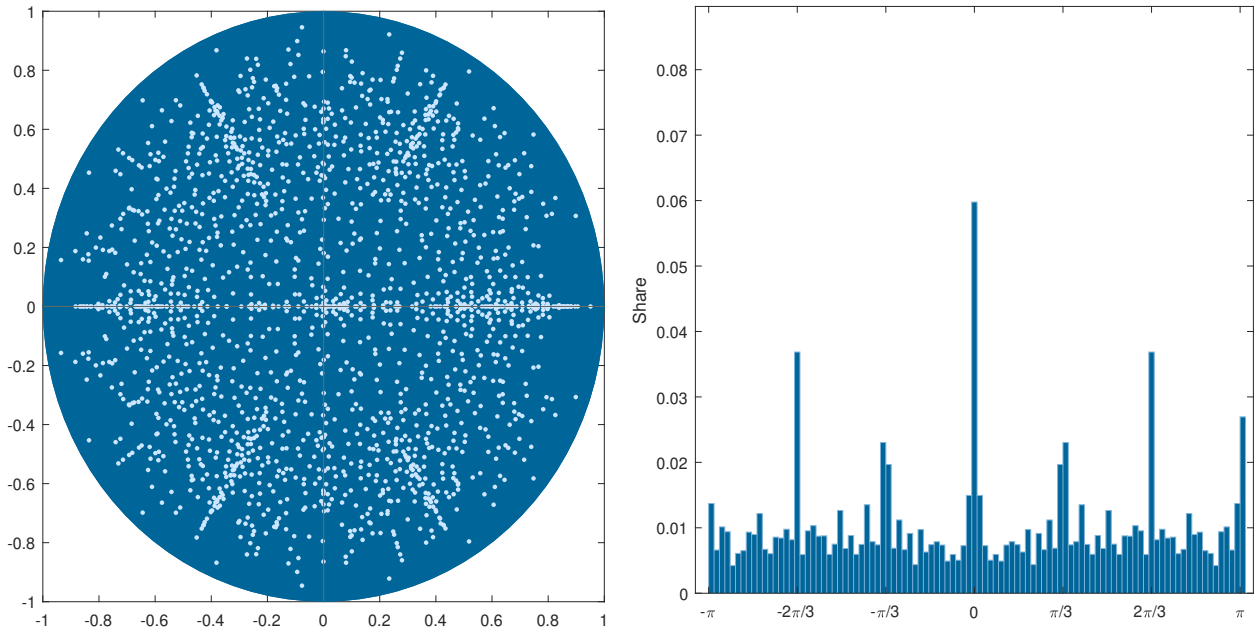

Notes: The left panel displays the eigenvalue spectrum of matrix $\mathbf{O}$ in the complex plane for the model with heterogeneous time-to-build, computed at the monthly frequency with Compustat data. The right panel shows the angular frequency distribution of those eigenvalues in radian, weighted by their norms.

Figure 14: Eigenvalue spectrum and angular frequency distribution

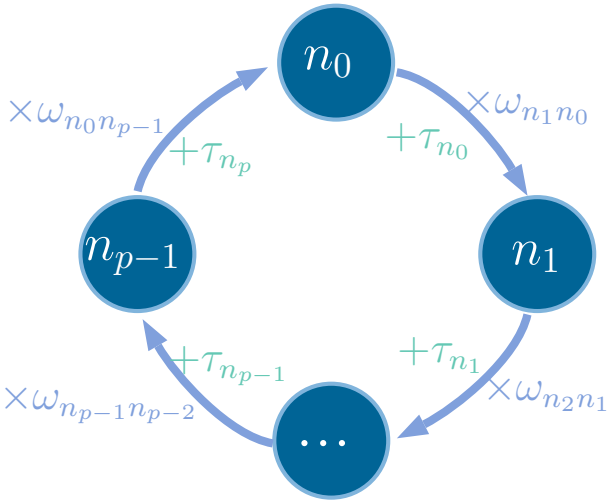

Figure 15: Propagation of shocks in a directed cycle

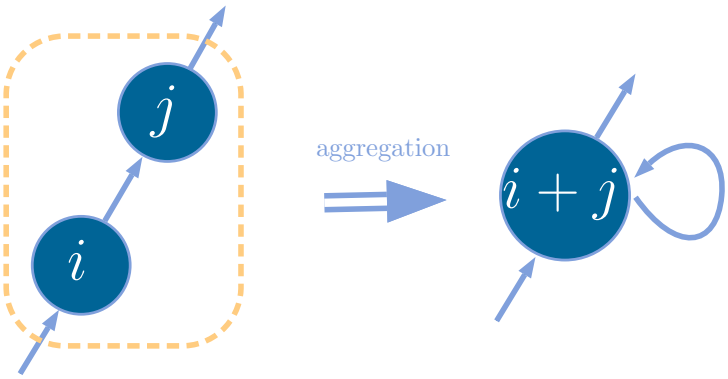

Notes: In this example, there are two sectors organized in a purely downstream production network without cycles. In this hypothetical situation, sector j buys intermediate inputs from sector i but sector i does not buy anything from sector j. If sectors i and j were to be aggregated in the same sector, the input-output matrix would indicate a self-loop for the joint sector $i + j$, falsely indicating the existence of a directed cycle in production and leading to erroneous conclusions for the cyclical properties of the economy.

Figure 16: Aggregation bias

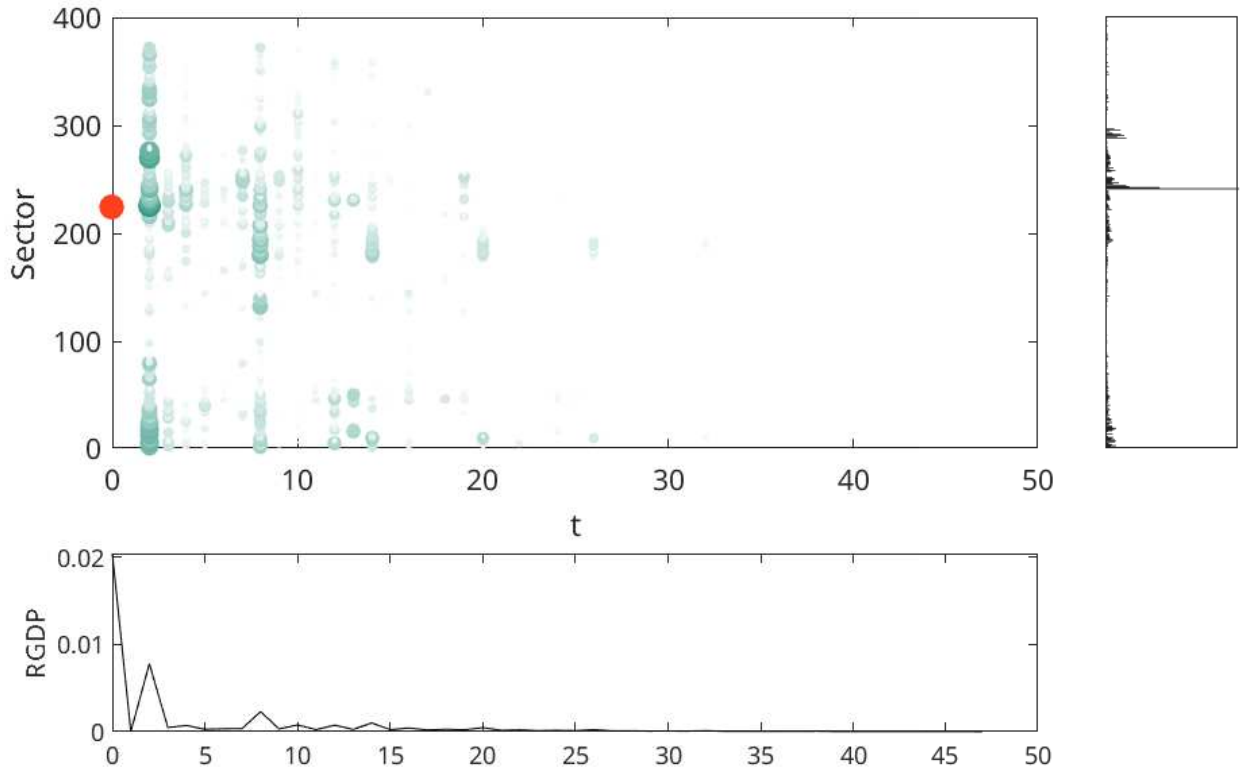

Notes: Shock normalized to 1%. Initial shock to sector 225 indicated in red at $t = 0$. The magnitude of the impact in each sector is represented by the size and darkness of the dot. We use a logarithmic color scale to highlight the propagation of the shock. The x-axis represents time in months, the y-axis corresponds to an internal sectoral index for the 372 sectors that we consider. The right panel is a weighted histogram of the cumulated impact of the shock in each sector. The bottom panel displays the response of aggregate GDP in percentage terms.

Figure 17: Sector #334110 - Petroleum Refineries

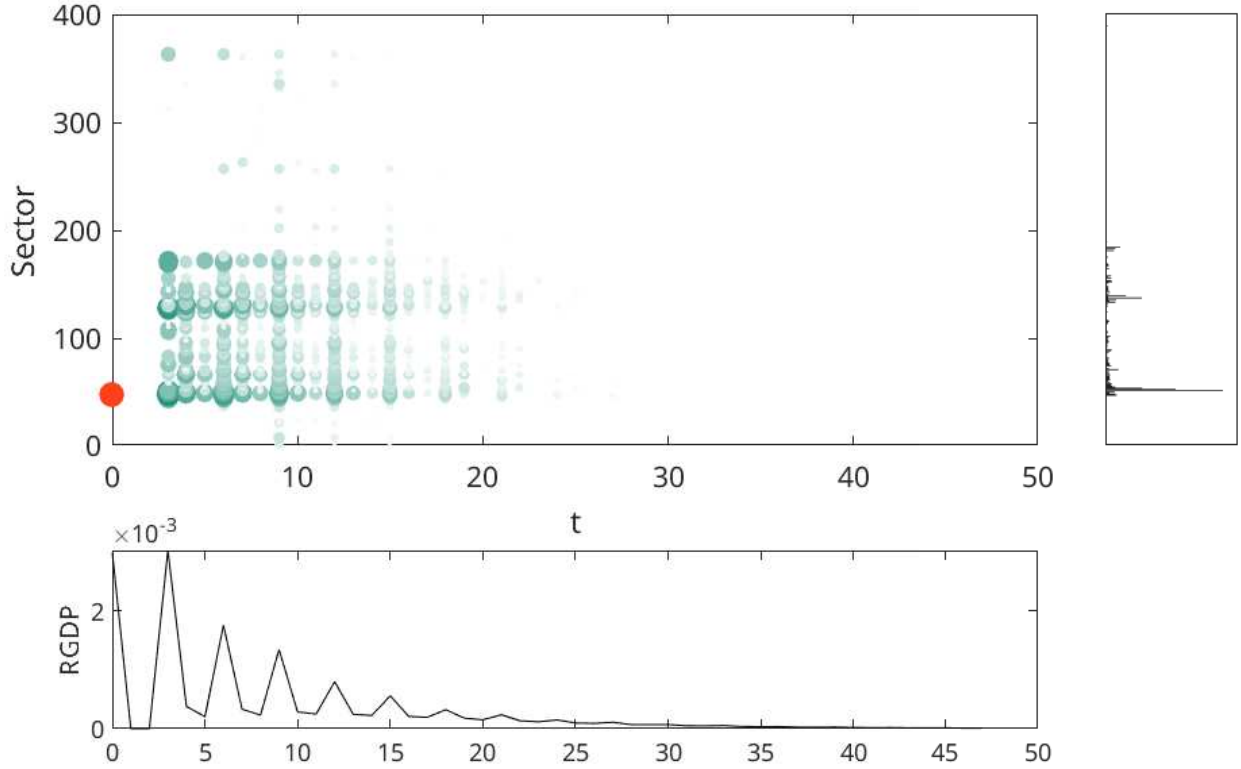

Notes: Shock normalized to 1%. Initial shock to sector 47 indicated in red at $t = 0$. The magnitude of the impact in each sector is represented by the size and darkness of the dot. We use a logarithmic color scale to highlight the propagation of the shock. The x-axis represents time in months, the y-axis corresponds to an internal sectoral index for the 372 sectors that we consider. The right panel is a weighted histogram of the cumulated impact of the shock in each sector. The bottom panel displays the response of aggregate GDP in percentage terms.

Figure 18: Sector #331410 - Nonferrous metal (...)

B Proofs

Proposition 1. *Under assumptions (6) and (7), the planner's value function can be expressed as*

$$V\left(\{A_n\}_{n=1}^N, \{X_{1\tau}\}_{\tau=0}^{\tau_1-1}, \ldots\right) = \sum_{n=1}^{N}\sum_{\tau=0}^{\tau_n-1}\beta^\tau \zeta_n \log X_{n\tau} + G\left(\{A_n\}_{n=1}^N\right) + \kappa$$

where

$$\boldsymbol{\zeta} = \left(\mathbf{I} - [\boldsymbol{\Omega}\boldsymbol{diag}(\beta^{\boldsymbol{\tau}})]'\right)^{-1}\boldsymbol{\gamma} \tag{28}$$

$$G\left(\{A_n\}_{n=1}^N\right) = \sum_n \beta^{\tau_n}\zeta_n \log A_n + \beta E\left[G\left(\{A'_n\}_{n=1}^N\right)\right] \tag{29}$$

and the allocation satisfies

$$\begin{aligned} c_n &= \overline{c_n} X_{n0} \\ x_{nm} &= \overline{x_{nm}} X_{no} \\ l_n &= \overline{l_n}, \end{aligned}$$

where

$$\begin{aligned} \overline{c}_n &= \gamma_n/\zeta_n \\ \overline{x}_{nm} &= \omega_{nm}\beta^{\tau_n}\zeta_n/\zeta_m \\ \overline{l}_n &= \alpha_n\beta^{\tau_n}\zeta_n/\left(\sum_m \alpha_m\beta^{\tau_m}\zeta_m\right) \\ \kappa &= (1-\beta)^{-1}\left(\sum_n \gamma_n \log \overline{c}_n + \sum_n \beta^{\tau_n}\zeta_n \log \overline{l}_n^{\alpha_n}\prod_m \overline{x}_{nm}^{\omega_{nm}}\right). \end{aligned} \tag{30}$$

Proof. Derive the first-order conditions of the planning problem. Write the Lagrangian as

$$\mathscr{L} = \sum_n \gamma_n \log c_n + \sum_n p_n\left(X_{n0} - c_n - \sum_m x_{mn}\right) + w\left(1 - \sum l_n\right) + \beta E\left[V\left(\{A'_n\}_{n=1}^N, \{X'_{1\tau}\}_{\tau=0}^{\tau_1-1}, \ldots\right)\right],$$

where p_n is the Lagrange multiplier on good n's resource constraint (equal to the spot price of good n for immediate delivery in the decentralization) and w the multiplier on the time constraint (equal to the wage in the decentralization). The first order conditions are

$$[c_n] \quad \frac{\gamma_n}{c_n} = p_n \tag{31}$$

$$[x_{nm}] \quad p_m = \omega_{nm}\frac{y_n}{x_{nm}}\beta E\left[\frac{\partial V}{\partial X_{n,\tau_n-1}}\left(\{A'_n\}_{n=1}^N, \{X'_{1\tau}\}_{\tau=0}^{\tau_1-1}, \ldots\right)\right] \tag{32}$$

$$[l_n] \quad w = \alpha_n\frac{y_n}{l_n}\beta E\left[\frac{\partial V}{\partial X_{n,\tau_n-1}}\left(\{A'_n\}_{i=1}^N, \{X'_{1\tau}\}_{\tau=0}^{\tau_1-1}, \ldots\right)\right] \tag{33}$$

Taking the envelope condition over each state variable gives

$$[X_{n0}] \quad \frac{\partial V}{\partial X_{n0}} = p_n \tag{34}$$

$$[X_{n\tau}, \tau > 0] \quad \frac{\partial V}{\partial X_{n\tau}} = \beta E\left[\frac{\partial V}{\partial X_{n,\tau-1}}\left(\left\{A'_n\right\}_{n=1}^{N}, \left\{X'_{1\tau}\right\}_{\tau=0}^{\tau_1-1}, \ldots\right)\right] \tag{35}$$

We now proceed by guess and verify. Guess that the value function takes the form

$$V\left(\left\{A_n\right\}_{n=1}^{N}, \left\{X_{1\tau}\right\}_{\tau=0}^{\tau_1-1}, \ldots\right) = \sum_n \sum_{\tau=0}^{\tau_n-1} \zeta_{n\tau} \log X_{n\tau} + G\left(\left\{A_n\right\}_{i=1}^{N}\right) + \kappa, \tag{36}$$

where $\zeta_{n\tau}$ and κ are some unknowns and F some function to be determined later. With our guess, the envelope conditions (34) and (35) give

$$\frac{\partial V}{\partial X_{n0}} = \frac{\zeta_{n0}}{X_{n0}} = p_n \tag{37}$$

$$\frac{\partial V}{\partial X_{n\tau}} = \frac{\zeta_{n\tau}}{X_{n\tau}} = \beta E\left[\frac{\zeta_{n\tau-1}}{X_{n\tau}}\right] \Rightarrow \zeta_{n\tau} = \beta\zeta_{n\tau-1} \text{ for } \tau \geq 1. \tag{38}$$

Simplify the notation by introducing $\zeta_n \equiv \zeta_{n0}$. Given condition (38), we have $\zeta_{n\tau} = \beta^\tau \zeta_n$.

We now guess that consumption and intermediate inputs evolve in proportion to the aggregate stock of goods delivered today, that is,

$$c_n = \overline{c}_n X_{n0}$$
$$x_{nm} = \overline{x_{nm}} X_{no}$$

and that labor is fixed $l_n = \overline{l_n}$. Combining our guess with (31) and (37), we get

$$\frac{\zeta_n}{X_{n0}} = p_n = \frac{\gamma_n}{c_n} = \frac{\gamma_n}{\overline{c}_n X_{n0}} \Rightarrow \overline{c}_n = \frac{\gamma_n}{\zeta_n}.$$

Now combining (32) and (38), we get

$$p_m = \frac{\zeta_m}{X_{m0}} = \omega_{nm}\frac{y_n}{\overline{x}_{nm}X_{n0}}\beta E\left[\frac{\zeta_{m\tau_n-1}}{y_n}\right] = \omega_{nm}\frac{\beta^{\tau_n}\zeta_n}{\overline{x}_{nm}X_{n0}} \Rightarrow \overline{x}_{nm} = \omega_{nm}\frac{\beta^{\tau_n}\zeta_n}{\zeta_m}.$$

Using the condition that $\overline{c}_n + \sum_m \overline{x}_{mn} = 1$, we get

$$\frac{\gamma_n}{\zeta_n} + \sum_m \omega_{mn}\frac{\beta^{\tau_m}\zeta_m}{\zeta_n} = 1 \Rightarrow \zeta_n = \gamma_n + \sum_m \omega_{mn}\beta^{\tau_m}\zeta_m,$$

which we write in matrix form as

$$\boldsymbol{\zeta} = \boldsymbol{\gamma} + \left[\boldsymbol{\Omega}\mathbf{diag}\left(\beta^\tau\right)\right]'\boldsymbol{\zeta} \tag{39}$$

or in other words, we recognize expression (28): $\boldsymbol{\zeta} = \left(\mathbf{I} - \left[\boldsymbol{\Omega}\mathbf{diag}\left(\beta^{\boldsymbol{\tau}}\right)\right]'\right)^{-1}\boldsymbol{\gamma}$. Because $\boldsymbol{\Omega}$ is a matrix whose rows sum up to less than 1 and that $\beta < 1$, the matrix $\tilde{\boldsymbol{\Omega}} = \boldsymbol{\Omega}\mathbf{diag}\left(\beta^{\boldsymbol{\tau}}\right)$ has radius strictly less than 1 and $\mathbf{I} - \tilde{\boldsymbol{\Omega}}$ is invertible. The vector $\boldsymbol{\zeta}$ is thus well defined.

The optimality condition on labor gives

$$w = \alpha_n \frac{y_n}{l_n} \beta E\left[\beta^{\tau_n - 1} \frac{\zeta_n}{y_n}\right] \Rightarrow l_n = \alpha_n \beta^{\tau_n} \zeta_n / w.$$

Since labor must sum up to 1, derive an expression for the wage

$$1 = \sum_n l_n = \sum_n \alpha_n \beta^{\tau_n} \zeta_n / w \Rightarrow w = \sum_n \alpha_n \beta^{\tau_n} \zeta_n$$

and employment in sector i is $l_n = \alpha_n \beta^{\tau_n} \zeta_n / \left(\sum_m \alpha_m \beta^{\tau_m} \zeta_m\right)$.

We have thus found solutions for c_n, x_{nm} and l_n that satisfy our optimality conditions. We are left to verify that V satisfies the guess (36). We now show that guess (36) satisfies the Bellman equation after substituting the solutions for c_n, x_{nm} and l_n.

$$\begin{aligned}
&\sum_1^N \gamma_n \log c_n + \beta E\left[V\left(\left\{A'_n\right\}_{n=1}^N, \left\{X'_{1\tau}\right\}_{\tau=0}^{\tau_1 - 1}, \ldots, \left\{X'_{N\tau}\right\}_{\tau=0}^{\tau_N - 1}\right)\right] \\
=&\sum_1^N \gamma_n \log c_n + \beta E\left[\sum_n \sum_{\tau=1}^{\tau_n - 1} \beta^{\tau - 1} \zeta_n \log X_{n\tau} + \sum_n \beta^{\tau_n - 1} \zeta_n \log y_n + G\left(\left\{A'_n\right\}_{n=1}^N\right) + \kappa\right] \\
=&\sum_1^N \gamma_n \log c_n + \sum_n \beta^{\tau_n} \zeta_n \log y_n + \sum_n \sum_{\tau=1}^{\tau_n - 1} \beta^{\tau} \zeta_n \log X_{n\tau} + \beta E\left[G\left(\left\{A'_n\right\}_{n=1}^N\right)\right] + \beta\kappa
\end{aligned}$$

Substitute in the terms $c_n = \overline{c}_n X_{n0}$ and $y_n = A_n \overline{l}_n^{\alpha_n} \prod_m \left(\overline{x}_{nm} X_{m0}\right)^{\omega_{nm}}$, we collect the terms multiplying X_{n0} and identify them with the coefficient ζ_n:

$$\zeta_n = \gamma_n + \sum_m \beta^{\tau_m} \omega_{mn} \zeta_m,$$

which we recognize as condition (39). Collecting the terms multiplying the TFP terms, we get

$$G\left(\left\{A_n\right\}_{n=1}^N\right) = \sum_n \beta^{\tau_n} \zeta_n \log A_n + \beta E\left[G\left(\left\{A'_n\right\}_{n=1}^N\right)\right],$$

which recovers condition (29). Finally, collecting the terms belonging to the constant, we get

$$\kappa = \sum_1^N \gamma_n \log \overline{c}_n + \sum_n \beta^{\tau_n} \zeta_n \log \overline{l}_n^{\alpha_n} \prod_m \overline{x}_{nm}^{\omega_{nm}} + \beta\kappa,$$

which satisfies condition (30). We have thus verified that V satisfies the Bellman equation. Since

this equation is a standard contraction that satisfies the Blackwell sufficient condition, the proposed V is the unique solution. □

Lemma 1. *The coefficients ζ_n are equal to the consumption-time adjusted Domar weights,*

$$\zeta_n = \frac{p_{nt} y_{nt-\tau_n}}{VA_t},$$

where $VA_t = \sum_n p_{nt} c_{nt}$ is aggregate value added.

Proof. Consider a particular decentralization of the planning economy. Up to a scalar $\overline{p}_t$ that determines the nominal price level, each spot price p_{nt} (i.e., for immediate delivery) must be proportional to $p_n = \frac{\partial V}{\partial X_{n0}}$, the marginal social value of good n (see proof of Proposition 1):

$$p_{nt} = \overline{p}_t p_n = \overline{p}_t \frac{\zeta_n}{X_{n0}}.$$

In the decentralization, the household solves every period

$$\max_{c_n} \sum_n \gamma_n \log c_{nt},$$

subject to the budget constraint $\sum p_{nt} c_{nt} = w_t$. Furthermore, expenditure shares are fixed: $p_{nt} c_{nt} = \gamma_n w_t = \gamma_n VA_t$.

Define the consumption-time adjusted Domar weights as

$$\tilde{\zeta}_n \equiv \frac{p_{nt} y_{nt-\tau_n}}{VA_t}.$$

Substituting for the resource constraint on good n, we have

$$\tilde{\zeta}_n = \frac{p_{nt} \left(c_{nt} + \sum_m x_{mn,t} \right)}{VA_t} = \gamma_n + \frac{p_{nt} \sum_m x_{mn,t}}{VA_t}.$$

Recall from Proposition 1 that the FOC (32) can be written as

$$p_n = \omega_{mn} \frac{y_{mt}}{x_{mn,t}} \beta^{\tau_m} \frac{\zeta_m}{y_{mt}} = \omega_{mn} \frac{\beta^{\tau_m} \zeta_m}{x_{mn,t}}.$$

Hence,

$$\begin{aligned} \tilde{\zeta}_n &= \gamma_n + \frac{\overline{p}_t p_n \sum_m x_{mn,t}}{VA_t} \\ &= \gamma_n + \overline{p}_t \frac{\sum_j \omega_{mn} \beta^{\tau_m} \zeta_m}{VA_t}. \end{aligned}$$

We know from Proposition (1) that $c_{nt} = \frac{\gamma_n}{\zeta_n} X_{n0} = \frac{\gamma_n}{\zeta_n} y_{n,t-\tau_n}$, hence

$$VA_t = \sum_n p_{nt} c_{nt} = \overline{p}_t \sum_n \frac{\zeta_n}{y_{nt-\tau_n}} \frac{\gamma_n}{\zeta_n} y_{nt-\tau_n} = \overline{p}_t.$$

As a result, we obtain that the consumption-time adjusted Domar weight $\tilde{\zeta}_n$ satisfies

$$\tilde{\zeta}_n = \gamma_n + \sum_m \omega_{mn} \beta^{\tau_m} \zeta_m,$$

in which we recognize equation (39). We thus conclude that $\tilde{\zeta}_n = \zeta_n$. □

Proposition 2. *The average duration* $\mathcal{T}_{\mathbf{w}}\left(\hat{\mathbf{A}}\right)$ *for weighting vector* $\mathbf{w} > 0$ *is*

$$\mathcal{T}_{\mathbf{w}}\left(\hat{\mathbf{A}}\right) = \mathbf{w}' \boldsymbol{\Omega} \left(\mathbf{I} - \boldsymbol{\Omega}\right)^{-1} \boldsymbol{diag}\left(\boldsymbol{\tau}\right) \left(\mathbf{I} - \boldsymbol{\Omega}\right)^{-1} \hat{\mathbf{A}}.$$

Proof. Consider a shock to a single sector n, $\hat{\mathbf{A}} = \boldsymbol{\delta}_n = \begin{pmatrix} 0 & ... & 1 & ... & 0 \end{pmatrix}'$. Following the definition of $\mathcal{T}_{\mathbf{w}}$, we have

$$\mathcal{T}_{\mathbf{w}}\left(\boldsymbol{\delta}_n\right) = \underbrace{0}_{\substack{\text{contemporaneous} \\ \text{impact}}} + \underbrace{\tau_n \sum_m w_m \omega_{mn}}_{\substack{\text{duration of 1st round} \\ \text{through network}}} + \underbrace{\sum_m \left(\tau_n + \tau_m\right) \sum_l w_l \omega_{lm} \omega_{mn}}_{\text{duration of 2nd round}}$$
$$+ \underbrace{\sum_{m,l} \left(\tau_n + \tau_m + \tau_l\right) \sum_k w_k \omega_{kl} \omega_{lm} \omega_{mn}}_{\text{duration of 3nd round}} + ...$$

The average duration can be decomposed as the sum of the durations of all the walks through the network that start in sector n and end up in any other sector, each walk being weighted by the corresponding product of input shares (i.e., $\prod_{k=0}^{l-1} \omega_{n_{k+1} n_k}$ for the l-length walk $(n_0, n_1 ..., n_l)$).

Group the contributions of each round of production:

$$\mathcal{T}_{\mathbf{w}}\left(\boldsymbol{\delta}_n\right) = \Big(\underbrace{\sum_m w_m \omega_{mn}}_{\text{2nd round}} + \underbrace{\sum_m \sum_l w_l \omega_{lm} \omega_{mn}}_{\text{3rd round}} + ... \Big) \tau_n \quad \Big\} \begin{array}{l} \text{contribution of 1st round} \\ \text{to all further rounds} \end{array}$$
$$+ \sum_m \Big(\underbrace{\sum_l w_l \omega_{lm}}_{\text{3rd round}} + \underbrace{\sum_l \sum_k w_k \omega_{kl} \omega_{lm}}_{\text{4th round}} + ... \Big) \omega_{mn} \tau_m \quad \Big\} \begin{array}{l} \text{contribution of 2nd round} \\ \text{to all further rounds} \end{array}$$
$$+ ...$$

which can be rewritten in matrix form as

$$\begin{aligned}\mathcal{T}_{\mathbf{w}}(\boldsymbol{\delta}_n) &= \mathbf{w}'\left(\boldsymbol{\Omega}+\boldsymbol{\Omega}^2+\ldots\right)\tau_n\boldsymbol{\delta}_n \\ &+\sum_m \mathbf{w}'\left(\boldsymbol{\Omega}+\boldsymbol{\Omega}^2+\ldots\right)\tau_m\omega_{mni}\boldsymbol{\delta}_m \\ &+\sum_{m,l} \mathbf{w}'\left(\boldsymbol{\Omega}+\boldsymbol{\Omega}^2+\ldots\right)\tau_l\omega_{lm}\omega_{mn}\boldsymbol{\delta}_l+\ldots \\ &= \mathbf{w}'\boldsymbol{\Omega}\left(\mathbf{I}-\boldsymbol{\Omega}\right)^{-1}\left(\tau_n\boldsymbol{\delta}_n+\sum_m \tau_m\omega_{mn}\boldsymbol{\delta}_m+\sum_{m,l}\tau_l\omega_{lm}\omega_{mn}\boldsymbol{\delta}_l+\ldots\right)\end{aligned}$$

where we have used the Leontief inverse $(\mathbf{I}-\boldsymbol{\Omega})^{-1}=\mathbf{I}+\boldsymbol{\Omega}+\boldsymbol{\Omega}^2+\ldots$. Replace each of the terms $\tau_m\boldsymbol{\delta}_m$ by $\mathbf{diag}(\boldsymbol{\tau})\boldsymbol{\delta}_m$ and obtain

$$\mathcal{T}_{\mathbf{w}}(\boldsymbol{\delta}_n)=\mathbf{w}'\boldsymbol{\Omega}\left(\mathbf{I}-\boldsymbol{\Omega}\right)^{-1}\mathbf{diag}(\boldsymbol{\tau})\left(\boldsymbol{\delta}_n+\sum_m\omega_{mn}\boldsymbol{\delta}_m+\sum_{m,l}\omega_{lm}\omega_{mn}\boldsymbol{\delta}_l+\ldots\right).$$

We recognize in the final term in the parenthesis the sum of all weighted walks of any length from n to any other sector. This can be rewritten as

$$\begin{aligned}\mathcal{T}_{\mathbf{w}}(\boldsymbol{\delta}_n) &= \mathbf{w}'\boldsymbol{\Omega}\left(\mathbf{I}-\boldsymbol{\Omega}\right)^{-1}\mathbf{diag}(\boldsymbol{\tau})\left(\mathbf{I}+\boldsymbol{\Omega}+\boldsymbol{\Omega}^2+\ldots\right)\boldsymbol{\delta}_n \\ &= \mathbf{w}'\boldsymbol{\Omega}\left(\mathbf{I}-\boldsymbol{\Omega}\right)^{-1}\mathbf{diag}(\boldsymbol{\tau})\left(\mathbf{I}-\boldsymbol{\Omega}\right)^{-1}\boldsymbol{\delta}_n.\end{aligned}$$

The general case for a shock $\hat{\mathbf{A}}=\sum\hat{A}_n\boldsymbol{\delta}_n$ follows by linearity. □

Proposition 3. *The marginal impact of a delay shock $\partial\tau_{in}$ on the persistence of shock $\hat{\mathbf{A}}$ is given by the product of supplier and buyer centrality measures:*

$$\partial\mathcal{T}_{\mathbf{w}}\left(\hat{\mathbf{A}}\right)/\partial\tau_n=s_n\times b_n,$$

where $b_n=\hat{\mathbf{A}}'\left(\mathbf{I}-\boldsymbol{\Omega}'\right)^{-1}\boldsymbol{\delta}_n$ is a shock $\hat{\mathbf{A}}$-weighted measure of sector n's buyer centrality, and $s_n=\tilde{\mathbf{w}}'\left(\mathbf{I}-\boldsymbol{\Omega}\right)^{-1}\boldsymbol{\delta}_n$ is a vector $\tilde{\mathbf{w}}$-weighted measure of sector n's supplier centrality, where $\tilde{\mathbf{w}}=\boldsymbol{\Omega}'\mathbf{w}$.

Proof. The proof is straightforward. Consider the derivative of $\mathcal{T}_{\mathbf{w}}$ with respect to τ_n:

$$\frac{\partial\mathcal{T}_{\mathbf{w}}}{\partial\tau_n}\left(\hat{\mathbf{A}}\right)=\mathbf{w}'\boldsymbol{\Omega}\left[\mathbf{I}-\boldsymbol{\Omega}\right]^{-1}\frac{\partial\mathbf{diag}(\boldsymbol{\tau})}{\partial\tau_n}\left[\mathbf{I}-\boldsymbol{\Omega}\right]^{-1}\hat{\mathbf{A}}.$$

$\partial\mathbf{diag}(\boldsymbol{\tau})/\partial\tau_n$ is an $N\times N$ matrix filled with 0s whose $(n,n)\,th$ element is 1, hence $\partial\mathbf{diag}(\boldsymbol{\tau})/\partial\tau_n=$

$\boldsymbol{\delta}_n \boldsymbol{\delta}_n'$. Hence,

$$\frac{\partial \mathcal{T}_{\mathbf{w}}}{\partial \tau_n}\left(\hat{\mathbf{A}}\right) = \mathbf{w}'\boldsymbol{\Omega}\left[\mathbf{I}-\boldsymbol{\Omega}\right]^{-1}\boldsymbol{\delta}_n\boldsymbol{\delta}_n'\left[\mathbf{I}-\boldsymbol{\Omega}\right]^{-1}\hat{\mathbf{A}}.$$

Grouping terms, the marginal impact appears as the product of two real numbers:

$$\begin{aligned}\frac{\partial \mathcal{T}_{\mathbf{w}}}{\partial \tau_n}\left(\hat{\mathbf{A}}\right) &= \left[\mathbf{w}'\boldsymbol{\Omega}\left[\mathbf{I}-\boldsymbol{\Omega}\right]^{-1}\boldsymbol{\delta}_n\right] \times \left[\boldsymbol{\delta}_n'\left[\mathbf{I}-\boldsymbol{\Omega}\right]^{-1}\hat{\mathbf{A}}\right] \\ &= \left[\mathbf{w}'\boldsymbol{\Omega}\left[\mathbf{I}-\boldsymbol{\Omega}\right]^{-1}\boldsymbol{\delta}_n\right] \times \left[\hat{\mathbf{A}}'\left[\mathbf{I}-\boldsymbol{\Omega}'\right]^{-1}\boldsymbol{\delta}_n\right] \\ &= s_n \times b_n,\end{aligned}$$

delivering the desired expression. The interpretation of both terms as centrality measures is provided in the main text. □

Proposition 4. *If productivity shocks are i.i.d., a $p-$cycle $\varsigma = (n_0, n_1, \ldots, n_{p-1}, n_p = i_0)$ contributes (at least) to the ACF of sector n_0:*

$$\gamma_{k\tau(\varsigma)}(n_0) = w(\varsigma)^{|k|}\,\sigma^2(\hat{y}_{n_0 t})$$

for $k \in \mathbb{N}$ and to the Fourier spectrum

$$f_{n_0}(\omega) = \frac{\sigma^2(\hat{y}_{n_0 t})}{2\pi}\frac{1-w(\varsigma)^2}{1+w(\varsigma)^2-2w(\varsigma)\cos(\omega\tau(\varsigma))},$$

where $\sigma(\hat{y}_{n_0,t})$ is the standard deviation of $\hat{y}_{n_0 t}$, $\tau(\varsigma)$ is the duration and $w(\varsigma)$ the weight of cycle ς.

Proof. As explained in the main text, all the shocks that hit sector n_0 at time t, whose total variance is $\sigma^2(\hat{y}_{n_0 t})$, propagate along the cycle and reappear every $k\times\tau(\varsigma)$ periods later, scaled by $w(\varsigma)^k$. As a result, the ACF of sector n_0 is at least

$$\gamma_{k\tau(\varsigma)}(n_0) = E\left[\hat{y}_{nt}\hat{y}_{n,t-k\tau(\varsigma)}\right] = w(\varsigma)^k\,\sigma^2(\hat{y}_{n_0 t}),$$

for $k = 0, \ldots, \infty$. Since $\hat{y}_{nt}$ is stationary, we have that $\gamma_k(n_0) = \gamma_{-k}(n_0)$, yielding the desired expression.

The Fourier transform based on this lower estimate of the ACF is

$$\begin{aligned} f_{n_0}(\omega) &= \frac{1}{2\pi}\sum_{k=-\infty}^{\infty}\gamma_{k\tau}(n_0)\, e^{-i\omega k\tau(\varsigma)} \\ &= \frac{\sigma^2(\hat{y}_{n_0 t})}{2\pi}\left(1+\sum_{k=1}^{\infty} w(\varsigma)^k\left(e^{i\omega k\tau}+e^{-i\omega k\tau}\right)\right) \\ &= \frac{\sigma^2(\hat{y}_{n_0 t})}{2\pi}\left(\frac{1}{1-we^{i\omega\tau}}+\frac{1}{1-we^{-i\omega\tau}}-1\right) \\ &= \frac{\sigma^2(\hat{y}_{n_0 t})}{2\pi}\left(\frac{1-w^2}{1+w^2-2w\cos(\omega\tau)}\right). \end{aligned}$$

□

Proposition 5. *The Fourier spectrum of aggregate real GDP is given by*

$$f_y(\omega) = \sum_{n=1}^{N}\mu_n^2 f_n(\omega) + \frac{1}{2\pi}\sum_{n\neq m}\sum_{k=-\infty}^{\infty}\mu_n\mu_m\left[\mathbf{\Gamma}_k\right]_{nm} e^{-i\omega k}.$$

Proof. The density spectrum of aggregate GDP is given by

$$\begin{aligned} f_y(\omega) &= \frac{1}{2\pi}\sum_{k=-\infty}^{\infty} E\left[\hat{y}_t\hat{y}_{t-k}\right] e^{-i\omega k} \\ &= \frac{1}{2\pi}\sum_{n=1}^{N}\sum_{k=-\infty}^{\infty}\mu_n^2\gamma_k(n)\, e^{-i\omega k} + \frac{1}{2\pi}\sum_{n\neq m}\sum_{k=-\infty}^{\infty}\mu_n\mu_m\left[\mathbf{\Gamma}_k\right]_{n,m} e^{-i\omega k}. \end{aligned}$$

We recognize in the first term a weighted sum of each sector's Fourier spectrum, while the second term shows the contribution of sectoral comovements. In other words,

$$f_y(\omega) = \sum_{n=1}^{N}\mu_n^2 f_n(\omega) + \frac{1}{2\pi}\sum_{n\neq m}\sum_{k=-\infty}^{\infty}\mu_n\mu_m\left[\mathbf{\Gamma}_k\right]_{n,m} e^{-i\omega k}.$$

□